

UPDATE ON NHTSA'S OMDB'S HALF BARRIER ANALYSIS

James Saunders
Dan Parent
NHTSA
USA

Paper Number 23-0314

ABSTRACT

Research Question/Objective: National Highway Traffic Safety Administration (NHTSA) has developed an Oblique Offset Moving Deformable Barrier (OMDB) test procedure. The OMDB test procedure uses an energy absorbing honeycomb that covers the front face of the OMDB. Originally, this barrier had a full-width design that was representative of a typical passenger car. During the development of this test procedure, it was realized that less than half of the barrier face was being deformed. Since only half the honeycomb was being deformed it was determined this was a waste of material and added cost to perform the test. Also, it was brought to NHTSA's attention that the manufacturing of the full-width barrier face was complicated by the need for straps. Therefore, NHTSA is developing a barrier with a face whose width is about half of the original. It is referred to as the "Half Barrier." Two different versions of the Half Barrier design, V0 and V1, are investigated herein.

Methods and Data Sources: The Full, Half V0, and Half V1 barrier faces were tested using the OMDB test procedure with rigid moving barrier and production vehicles, representing different size vehicles. In each test with production vehicles, THOR-50M Anthropomorphic Test Devices (ATDs) were positioned in the driver and right front passenger seat. Differences in barrier, vehicle, and occupant response were assessed using CORA rating software. To eliminate the variability of production vehicles a set of tests using a rigid moving barrier was used as the target vehicle. Differences in barrier, vehicle, and occupant response were assessed using CORA.

Results: The impacts into the rigid moving barrier showed a "Good" CORA score for the rigid moving barrier responses, though the barrier crush and energy had different trends. In the production vehicle tests, some differences were seen in the vehicle crash pulses and intrusions when comparing different barrier faces within the same vehicle. For example, the large pickup truck showed a more severe crash pulse using the Half V1 barrier face, suggesting that V1 is stiffer than the other barrier faces

Discussion and Limitations: During this testing it was noted that the two layers of honeycomb had a slight separation. This separation was seen in the full-width barrier and both designs of the Half Barrier. It is unknown how much this separation affects the vehicle and ATD response. This study was limited by the number of observations, as only one test was conducted for each barrier face/vehicle combination, and only three production vehicles were tested. However, the range of vehicles was selected to cover a wide range of characteristics.

Conclusions and Relevance to Session Submitted: The Half V0 barrier face design has been tentatively selected as a replacement for the full-width barrier for use in NHTSA's OMDB test procedure. It shows comparable results to the full-width barrier for both the vehicle and THOR-50M performance. The Half Barrier V1 design seemed to be too stiff for larger vehicles.

INTRODUCTION

National Highway Traffic Safety Administration (NHTSA) has developed an Oblique Offset Moving Deformable Barrier (OMDB) test procedure. The OMDB test procedure uses an energy absorbing honeycomb that covers the front face of the OMDB. This barrier is referred to as "Full" (Figure 1) [1]. During the development of this test procedure, it was realized that less than half of the barrier face was being deformed. Since only half the honeycomb was being deformed, it was determined this was a waste of material and added extra cost to perform the test.

HALF-BARRIER DESIGNS

Two versions of a half-barrier are explored herein:

Half-barrier version V0: This version was designed to be a smaller and more simplistic version of the Full barrier. For the Full barrier, it was noted that the manufacturing of the barrier face is complicated by the use of strapping. Therefore, the barrier face width was reduced by about half and outer cladding was made from one piece of metal, eliminating the need to rivet and allowing the straps and the side cladding to be removed. The resulting barrier face is referred to as “Half V0” (Figure 2) [2]. To eliminate the movement of the honeycomb from deforming toward the outer edge of the OMDB a support was added (*Figure 5*) (Appendix A). It should be noted that the honeycomb is not connected to the support. The support was designed to composite for the difference in mass between the honeycombs

Half-barrier version V1: It was noted after performing tests with Half V0 that the honeycomb layers were separating for both Full and Half V0. This separation was noted by looking at pictures from previous tests. Separation included both delamination and the honeycomb sliding relative to each other. *Figure 4* shows an example of barrier separation for the Full barrier. The front honeycomb is lower compared to the back honeycomb and there is a gap between the two pieces of honeycomb. Also, it was noted that the interior edge of the Half V0 face was expanding out from the barrier, whereas at the same location for the Full barrier it stayed the same (*Figure 5*). Again, it is unknown if all tests had separation since the barrier faces were not available to investigate. While it is not known how the honeycomb separation affects the test results, the initial perception was that the separation could present reproducibility concerns. Therefore, another version of the half-barrier face was designed in an attempt to prevent the separation from occurring. This version is referred to as “Half V1.” The medial end of the cladding was fixed to the barrier and the lateral end of the barrier was capped (Figure 3).

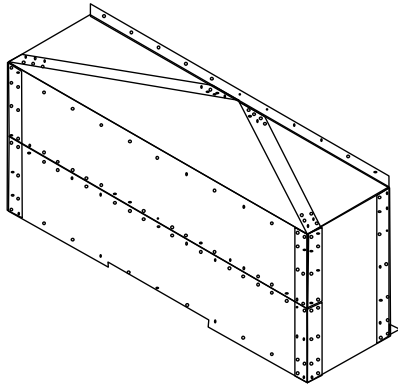


Figure 1 Original barrier face (Full)

- Width slightly > 50%
- Same materials
- Removed straps, rivets, side cladding
- One-piece outer cladding

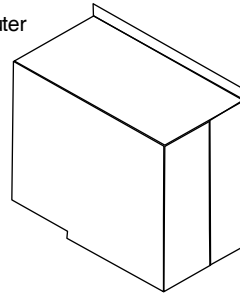


Figure 2 1st version reduced face design (Half V0)

- Medial end of cladding fixed to barrier
- Lateral end of barrier capped

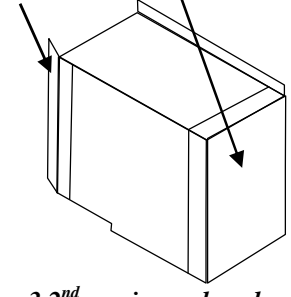


Figure 3 2nd version reduced face design (Half V1)

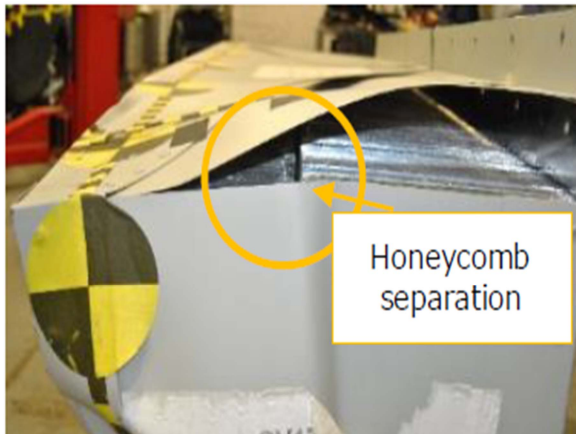


Figure 4 Example of Full honeycomb separation

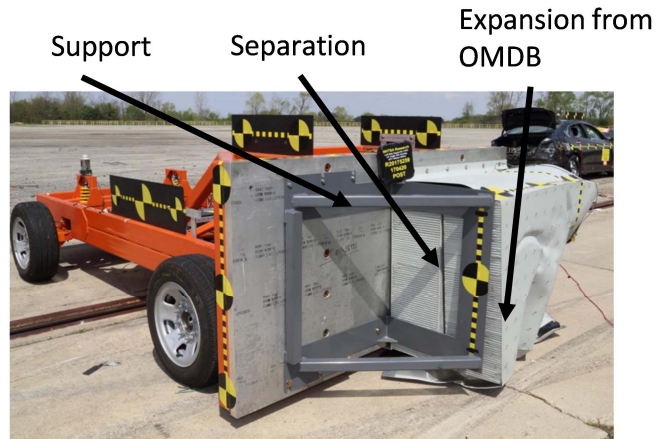


Figure 5 Picture showing extra support added for half barrier design and honeycomb separation

Saunders [3] demonstrated that the OMDB, vehicle, and Test Device for Human Occupant Restraint 50th percentile male (THOR-50M) responses in the OMDB test procedure were repeatable and reproducible. For the half barrier to be used, it needs to be demonstrated that the results from the half barrier test are equivalent to those from the full barrier test. This report follows the same methodology as Saunders [3].

METHODOLOGY

Test Setup

Figure 6 shows the general test setup for the OMDB crash test. The OMDB impacts the target vehicle at a test speed of 90 km/h at a 15-degree offset and at 35 percent overlap of the target vehicles' overall width (excluding mirrors and door handles). The outer edge of the OMDB is aligned with the overlap mark on the target vehicle.

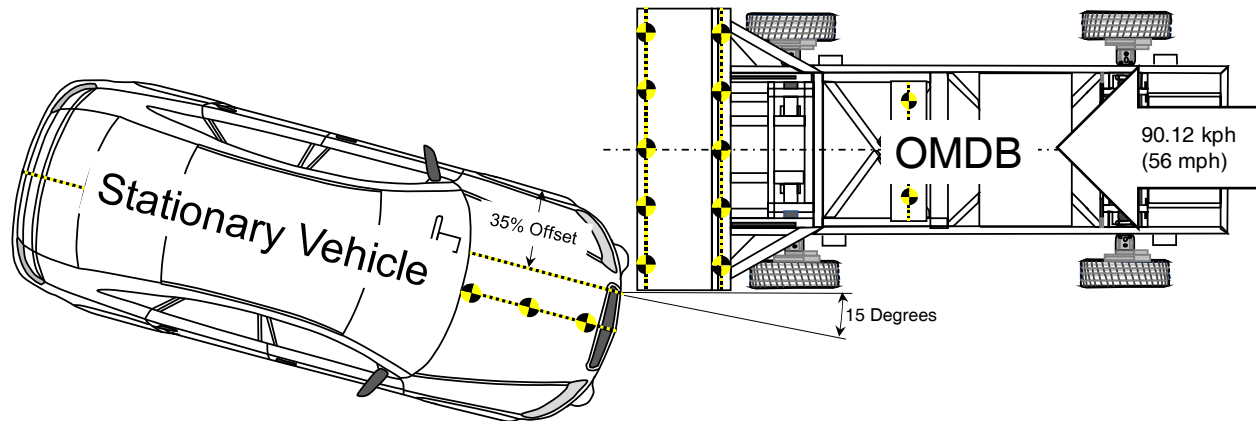


Figure 6 OMDB test setup

Vehicle Selection

The production vehicles selected for this testing were intended to cover a range of vehicle sizes. Table 1 shows the naming convention used for this analysis and the NHTSA test numbers for each test [4]. To determine if the Half V1 version prevented honeycomb separation only the Small and Large PU tests were performed. If Half V1 prevented honeycomb separation than additional vehicles would be tested.

Table 1
Vehicle naming convention and relative NHTSA test numbers

Vehicle Type	NHTSA Test Number		
	Half V0	Half V1	Full
Small	10134	10824	10133
Mid-size	10072	NA	10154
Large PU	10119	10825	10099

Honeycomb Crush

To measure the crush of the honeycomb, the barrier face was divided by ten evenly spaced horizontal lines relative to the vertical axis of the OMDB (R1 through R10) (Figure 7). Post-test the crush was measured along these horizontal lines, i.e., holding at the same z-height as pre-test. The lab measured enough points along each horizontal line to represent the deformation. It should be noted that the plots of barrier crush throughout the paper only show the same portion of the Full barrier that overlaps the half barrier. Also, R3, R6, and R9 crush measurements are used to get a representation of the crush throughout the barrier.

This barrier crush was used to calculate the energy absorbed by the honeycomb. To calculate the energy, the honeycomb was assumed to be the same constant stiffness as the first layer of honeycomb. While there are two layers of honeycomb with different stiffnesses, this assumption was made because the crush into the second layer was seen to be less than 50 mm. The Equation 1 shows the equation used to calculate the energy absorbed by the honeycomb during the test.

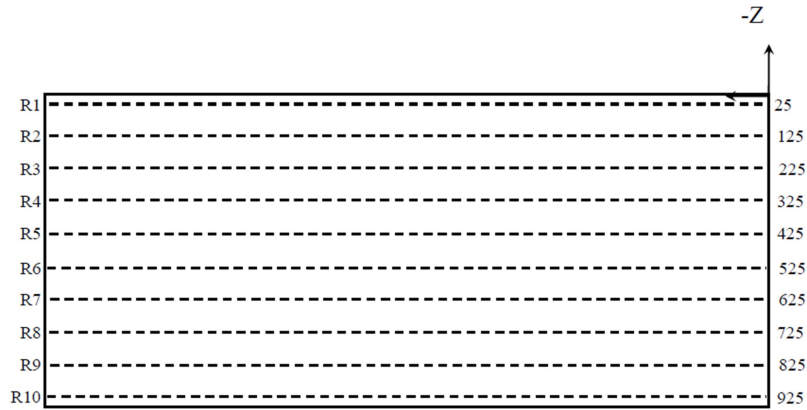


Figure 7 Barrier crush measurements

$$energy (kJ) = \frac{V}{k * 1000 * 1000 * 1000 * 1000} \quad (1)$$

V = crushed honeycomb volume (mm^3)

k = crush strength of first layer of honeycomb (689475.729 psi)

Vehicle Interior Intrusions

For all tests, pre- and post-test measurements were collected from the interior of the test vehicles following the OMDB procedure [5]. Figure 6 shows the location of each of these points.

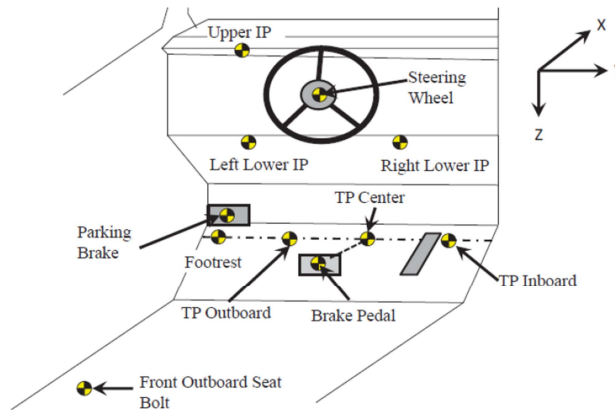


Figure 6 Driver side interior pre- and post-test points

Objective Evaluation

CORrelation and Analysis (CORA) [6] provides a methodology to objectively compare the time histories of the measurements and quantify how two or more signals compare on a scale of 0 to 1, where a higher total CORA score represents a higher correlation between each test or measurement, and a score of 1 indicates that the signals are identical. CORA software uses two methods to evaluate the correlation of two or more signals: corridor and cross-correlation. The corridor method compares the deviation between curves, while the cross-correlation method compares curve characteristics such as shape, phase shift, and size.

For this analysis the CORA examples provided when downloading the CORA [5] were used. The only modification to these files was the reference to the time-history data and the time range for evaluation. As specified in the manual,

all data was sampled at 0.1 ms. CORA scores were calculated by assuming that the Full barrier test for each production vehicle was the experimental baseline, and the Half V0 and Half V1 tests (when available) were compared to this baseline. For this study, as in Saunders [3] **Error! Reference source not found.**, the time range used for calculation of CORA score was from 0 to 100 ms for the vehicle and OMDB time-histories, and from 0 to 200 ms for the occupant time-histories. The grading system presented in Saunders [3], which is divided into three categories based on CORA scores as shown in Table 2, was used in this study as well. Vehicle and OMDB time-histories used in the CORA analysis were selected to be able to compare vehicle and OMDB kinematics, accelerations, and velocities. Occupant response time-histories selected for CORA analysis were those used as input in the calculation of injury criteria for the THOR-50M ATD [3].

Table 2
CORA scores ranges

Grade	Calculated Score
Good	$R > 0.80$
Fair	$0.58 < R \leq 0.80$
Poor	$R \leq 0.58$

RESULTS

A total of 8 OMDB tests were conducted, with the closing speeds, impact angle, and vertical and lateral offset all within the specifications of the OMDB Laboratory Test Procedure (Table 3) [5]. Table 3 also shows the mass of Vehicle were similar between tests. There was a 82 kg difference in the mass of the OMDB. This is because not all tests were performed at the same test facility. Each facility had different equipment attached to the OMDB to pull it down the track. The moment of inertia and exact CG of the OMDB were not measured for any of these tests.

Table 3
Input parameters of the OMDB into production vehicles

Vehicle Description	Barrier	Closing Speed (kph)	OMDB Mass (kg)	Vehicle Mass (kg)	Angle (degrees)	Vertical Offset (mm)	Lateral Offset (mm)
Small	Full	90.79	2531.9	1574	15	-13	0
Small	Half V0	90.72	2518.5	1573	15	-3	2
Small	Half V1	89.62	2471	1572	14.5	8	48
Mid-size	Full	90.04	2450.2	1708.6	15	-14	-5
Mid-size	Half V0	90.33	2437	1717.8	15	-20	17
Large PU	Full	89.5	2462.3	2246.5	15.1	-12	-8
Large PU	Half V0	89.87	2451.2	2258	14.9	-16	10
Large PU	Half V1	90.12	2471	2272	15.2	-5	2

The remainder of the results section is presented in four subsections. The first describes the response of the OMDB itself, including both the kinematics of the moving barrier and the crush of the deformable honeycomb barrier faces. The second describes the response of the target vehicles, including kinematics, crush, and intrusion. The last two sections describe the response of the two occupants in each vehicle, the driver and the right front passenger.

OMDB Response

The magnitude of energy absorbed by the different honeycomb faces did not show any consistent trends across production vehicle sizes (Figure 8). The energy absorbed by the Half V0 for the Small and the Mid-size production vehicle decreased by 2.9 and 8.5 percent when compared to the Full barrier face, while the energy absorbed by the honeycomb for the Large PU increased by 13.8 percent. However, for the Half V1 barrier face, the energy absorbed

in the Small production vehicle increased by 12.2 percent compared to the Full barrier face, whereas the energy absorbed in the Large PU test decreased by 31.8 percent.

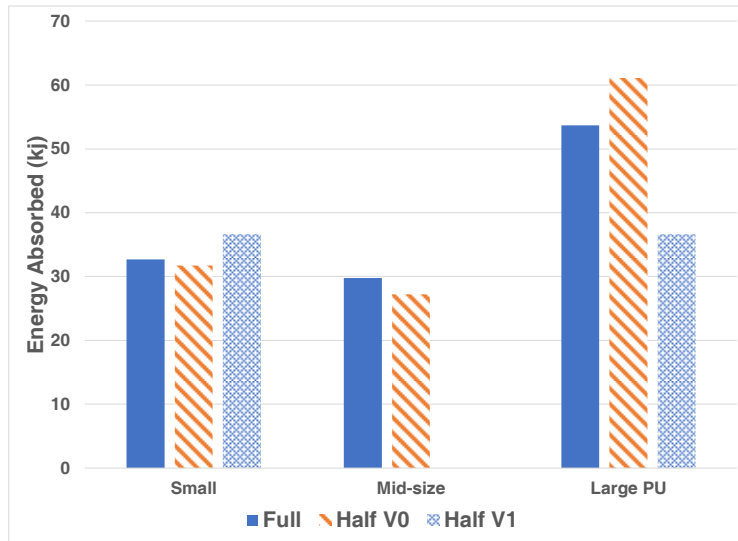


Figure 8 Energy absorbed by the honeycomb when the OMDB impacts production vehicles

Figure 9 through Figure 11 show the physical honeycomb crush for the Small production vehicle tests for comparison. Figure 12 through Figure 14 show the measured crush for R3, R6, and R9 for the Small production vehicle tests for comparison. Since the crush of the left half (-1200 to 0 mm), when looking from in front of the OMDB, of the Full honeycomb barrier face is negligible, only the common portions of the barrier faces (0 to +1200 mm) are shown. It is seen that the Half V0 expands away from the OMDB for all three rows and then is similar, except for R9. R9 followed the Full crush just after crush stopped expanding and then did not rise as high as the Full. The crush for R3 and R9 for Half V1 was shifted to the left at the beginning of crush and then had similar shape. R6 for Half V1 was similar, except for around 750 mm, it had more crush than both the Full and Half V0.



Figure 9 Picture of Full honeycomb crush for the OMDB impacting Small production vehicle



Figure 10 Picture of Half V0 honeycomb crush for the OMDB impacting Small production vehicle *



Figure 11 Picture of Half V1 honeycomb crush for the OMDB impacting Small production vehicle

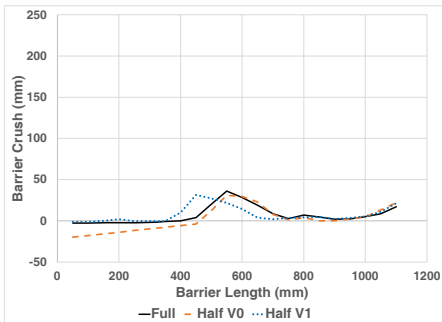


Figure 12 R3 honeycomb crush when impacting Small production vehicle

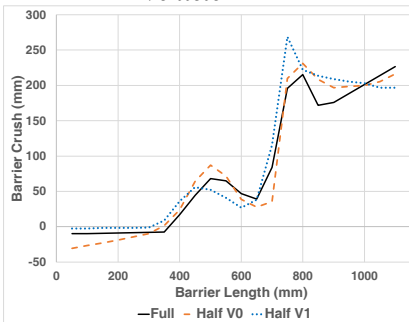


Figure 13 R6 honeycomb crush when impacting Small production vehicle

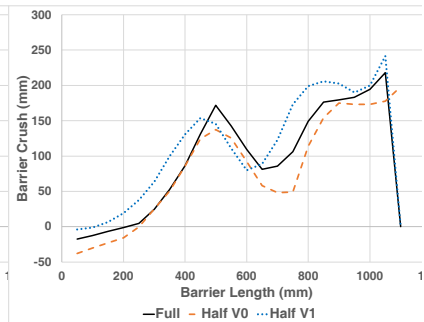


Figure 14 R9 honeycomb crush when impacting Small production vehicle

* Oblique picture not available

Figure 15 and Figure 16 show the physical honeycomb crush for the Mid-size production vehicle tests for comparison. Figure 17 through Figure 19 show the measured crush for R3, R6, and R9 for the Mid-size production vehicle tests for comparison. It is seen that the Half V0 expands away from the OMDB for all three rows and then is similar, except for the middle of the honeycomb. Each row does not crush as much as the Full.



Figure 15 Picture of Full honeycomb crush for the OMDB impacting Mid-size production vehicle



Figure 16 Picture of Half V0 honeycomb crush for the OMDB impacting Mid-size production vehicle

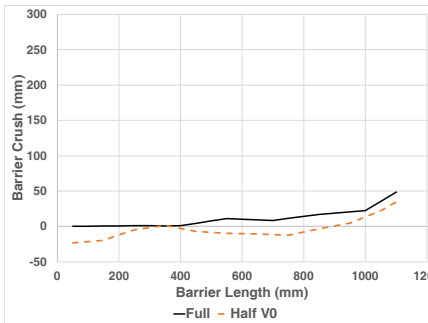


Figure 17 R3 honeycomb crush when impacting Mid-size production vehicle

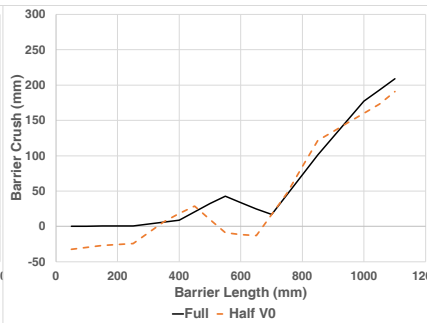


Figure 18 R6 honeycomb crush when impacting Mid-size production vehicle

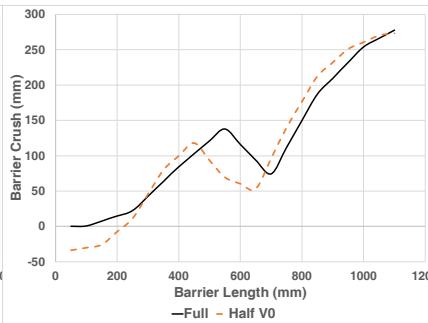


Figure 19 R9 honeycomb crush when impacting Mid-size production vehicle

Figure 20 through Figure 22 show the physical honeycomb crush for the Large PU tests for comparison. Figure 23 through Figure 25 show the measured crush for R3, R6, and R9 for the Large PU tests for comparison. It is seen that the Half V0 expands away from the OMDB for all three rows for the left side of the honeycomb. R3 crush was similar and R6 was similar up to 500 mm. R3 crush was less for the Half V1. Also, R6 was less up to 700 mm and then was greater for a short distance. R9 showed more crush than Full.



Figure 20 Picture of Full honeycomb crush for the OMDB impacting Large PU production vehicle



Figure 21 Picture of Half V0 honeycomb crush for the OMDB impacting Large PU production vehicle



Figure 22 Picture of Half V1 honeycomb crush for the OMDB impacting Large PU production vehicle

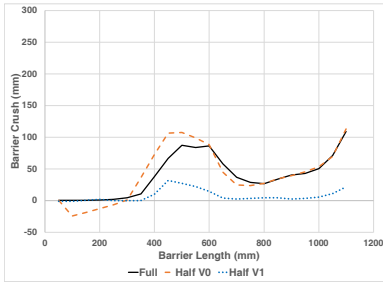


Figure 23 R3 honeycomb crush when impacting Large PU production vehicle

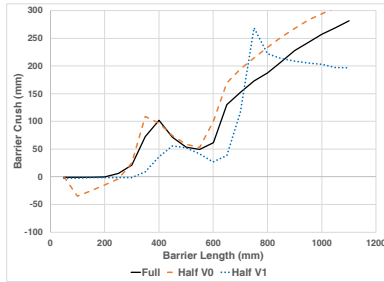


Figure 24 R6 honeycomb crush when impacting Large PU production vehicle

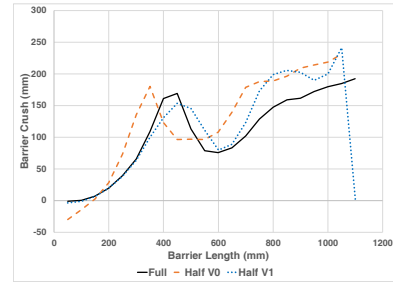


Figure 25 R9 honeycomb crush when impacting Large PU production vehicle

Table 4 shows the naming convention used throughout the paper for the time-histories of the OMDB measurements. Table 5 shows the CORA scores for the OMDB responses, which range from 0.884 to 1.000. Table 5 also shows that the average CORA score was greater than 0.95 for all vehicle sizes.

Table 4
Naming convention for OMDB time-histories

Name	Description
OMDBCGaccRes	OMDB CG resultant acceleration (x,y)
OMDBCGvelRes	OMDB CG resultant velocity (x,y)
OMDBCGav	OMDB CG angular velocity (z)
OMDBCGang	OMDB CG rotation (z)
OMDBRearAcc	OMDB Rear resultant acceleration (x,y)
OMDBRearVel	OMDB Rear resultant velocity (x,y)

Table 5
CORA scores for OMDB response when the OMDB impacts production vehicles

	Small		Mid-size		Large PU	
	V0	V1 ¹	V0	V1 ²	V0	V1
OMDBCGaccRes	0.993	0.942	0.968	NA	0.940	0.971
OMDBCGvelRes	0.998	0.976	0.998	NA	0.990	0.997
OMDBCGav	0.878	0.913	0.884	NA	0.931	0.956
OMDBCGang	0.960	0.989	0.941	NA	0.980	0.996
OMDBRearAcc	0.980	ND	0.987	NA	0.935	0.917
OMDBRearVel	0.997	ND	0.995	NA	0.993	0.986
Average	0.968	0.955	0.962	NA	0.962	0.971

ND – No data collected

NA – Not applicable, test was not performed for this vehicle

Vehicle Response

Figure 26 through Figure 28 show the bumper crush for each production vehicle when impacted by different honeycomb faces. The bumper crush for the Small production vehicle had similar shape for all honeycomb faces. The largest differences can be seen at the outer edge of the vehicle, where Half V0 had slightly more crush and Half V1 had slightly less crush than the Full barrier face. For the Mid-size vehicle, crush was similar for both barriers tested (Figure 27). For the Large PU, the bumper crush for the Half V0 is similar to the Full (Figure 28), except for minor differences at the outer edge of the vehicle. The Half V1, however, showed deviation from the Full barrier face at the outer edge of the vehicle, where crush was roughly 150 mm lower, and between 400 mm and 1200 mm of its profile, where there was more crush than both the Full and Half V0 barrier faces.

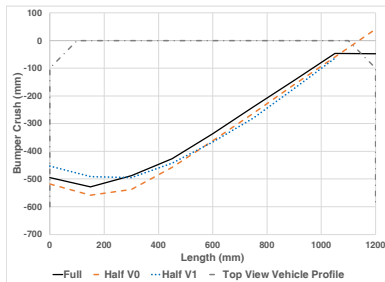


Figure 26 Bumper beam crush when the OMDB impacts Small production vehicle

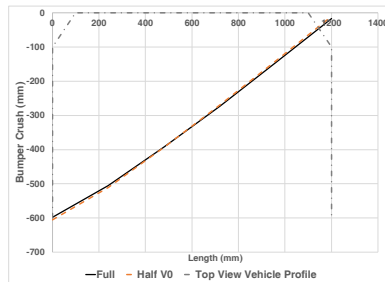


Figure 27 Bumper beam crush when the OMDB impacts Mid-size production vehicle

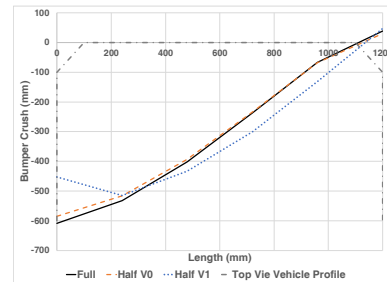


Figure 28 Bumper beam crush when the OMDB impacts Large-PU production vehicle

Figure 29 through Figure 31 show the interior intrusion for all production vehicles. The interior intrusions for the Small production vehicle were similar between the Half V0 and Full barrier tests (Figure 29), with the largest differences occurring in the TP Inboard and Brake Pedal measurement locations where the Half V0 intrusion was roughly 20 mm larger. Comparing the Half V1 and Full tests, the Half V1 resulted in about 80 mm more intrusion at the TP Footrest location, more intrusion at the Steering Wheel and Right Lower IP locations, and less intrusion at the Upper IP and Left Lower IP locations. The Mid-size production vehicle showed similar results when comparing Full versus Half V0 tests, except for the Brake Pedal location, where the Half V0 intrusion was 35 mm larger, and the Steering Wheel location, where Half V0 test showed 20 mm greater motion in the opposite direction. For the Large PU, the Half V0 test showed less intrusion than the Full barrier test in the Upper IP, Left Lower IP, and Brake Pedal locations. The Half V1 test showed more pronounced intrusion differences compared to Full and Half V0 tests (Figure 31), including 80 mm more intrusion at the TP Center location, 80-90 mm more intrusion at the TP Inboard

location, 40 mm more intrusion at the Right Lower IP location, and 20-40 mm less intrusion at the Brake Pedal location.

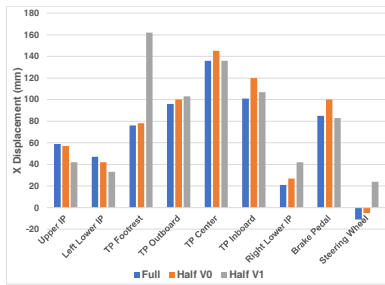


Figure 29 Interior points intrusions when the OMDB impacts Small production vehicle

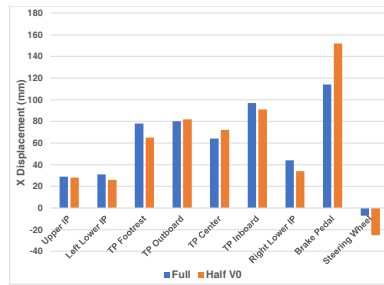


Figure 30 Interior points intrusions when the OMDB impacts Mid-size production vehicle

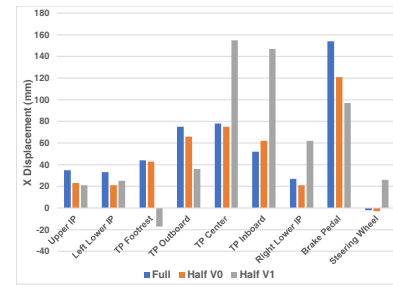


Figure 31 Interior points intrusions when the OMDB impacts Large-PU production vehicle

Table 6 shows the naming convention for the vehicle measurement time-histories. Table 7 shows that most of the CORA scores for the three production vehicles were rated “Good”. The VehLRaccRes for both V0 and V1 were rated “Fair” for the Large PU. The VehLRvelRes were rated “Good”. The scores for the VehCGav of all production vehicles were rated “Fair”, except for Large PU Half V0 which was “Good”. When integrating the angular velocity to get the rotation (VehCGang), it is seen that the CORA scores are rated “Good” for all the vehicles, except the Large PU.

Table 6

Naming convention for vehicle time-histories when a production vehicle is used as the target vehicle

Name	Description
VehLRaccRes	Test vehicle left rear sill resultant acceleration (x,y)
VehLRvelRes	Test vehicle left rear sill resultant velocity (x,y)
VehRRaccRes	Test vehicle right rear sill resultant acceleration (x,y)
VehRRvelRes	Test vehicle right rear sill resultant velocity (x,y)
VehCGaccRes	Test vehicle CG acceleration (x,y)
VehCGvelRes	Test vehicle CG resultant velocity (x,y)
VehCGav	Test vehicle CG angular velocity (z)
VehCGang	Test vehicle CG rotation (z)

Table 7
CORA scores for production vehicles response when the OMDB impacts production vehicles

	Small		Mid-size		Large PU	
	V0	V1	V0 ¹	V1 ²	V0	V1
VehLRaccRes	0.968	0.920	0.908	NA	0.798	0.702
VehLRvelRes	0.999	0.998	0.971	NA	0.988	0.993
VehRRaccRes	0.972	0.912	0.898	NA	0.860	0.915
VehRRvelRes	0.995	0.989	0.900	NA	0.991	0.996
VehCGaccRes	0.984	0.831	QD	NA	0.826	0.818
VehCGvelRes	1.000	0.978	QD	NA	0.978	0.969
VehCGav	0.636	0.734	0.719	NA	0.845	0.745
VehCGang	0.810	0.923	0.924	NA	0.991	0.681
Average	0.921	0.911	0.887	NA	0.910	0.852

QD – Questable data

NA – Not applicable, test was not performed for this vehicle

Figure 32 and Figure 33 show the left rear sill resultant acceleration of the Large PU when impacted by Half V0 and Half V1, respectively. Compared to the Full barrier test, the acceleration in the Half V0 test had a similar shape but a lower overall peak acceleration. The Half V1 test did not exhibit the rise in acceleration between 40 and 50 ms seen in the Full and Half V0 tests.

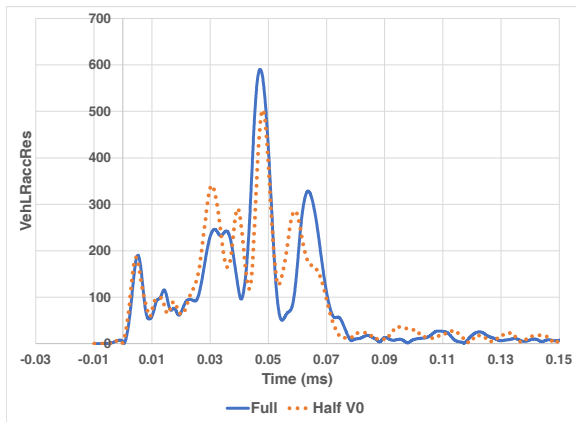


Figure 32 Left rear sill resultant acceleration for Large PU when impacted by Half V0 compared to Full

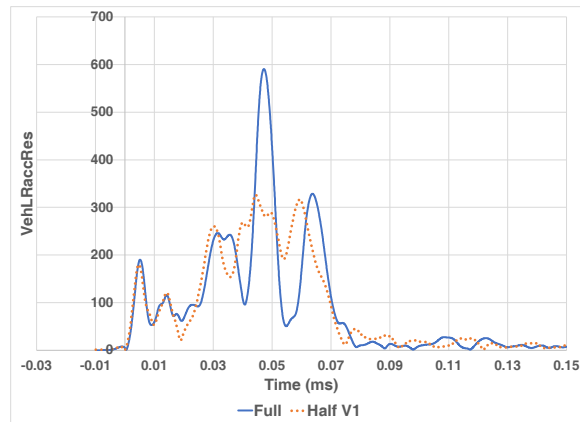


Figure 33 Left rear sill resultant acceleration for Large PU when impacted by Half V1 compared to Full

Figure 34 shows the integration of the angular velocity compared to film analysis for the Large PU Half V1. It is seen from film analysis that from 90 ms to 150 ms the rotations are similar, while the calculated angle keeps on diverging. Figure 35 zooms in on the film analysis between Full and Half V1. This is the time the two curves separate and then come back together. During this time the average difference was 0.31 degrees. It is interesting that this occurs about the same time as the difference in acceleration occurs (Figure 33).

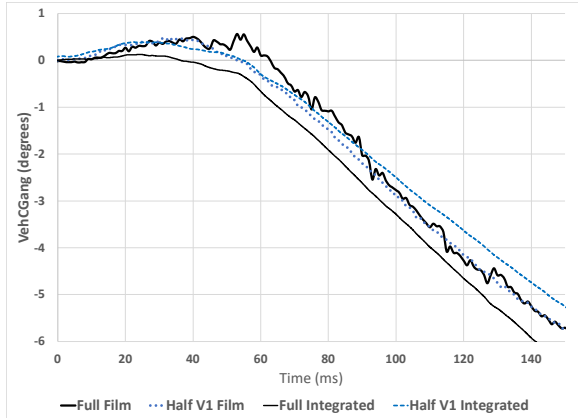


Figure 34 VehCGang from integrating VehCGav and film analysis for Large PU Half V1 compared to Full

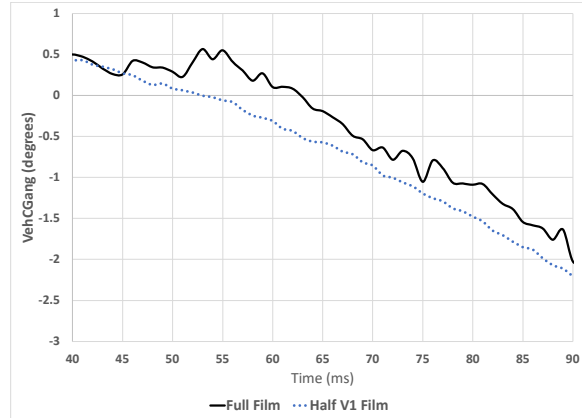


Figure 35 Zoom in on VehCGang from integrating VehCGav and film analysis for Large PU Half V1 compared to Full

Occupant Response: Driver

Within each production vehicle, driver kinematics were similar across all barrier designs. The minor differences that did occur are described in this section as they related to differences in occupant response time-histories. Table 8 shows the naming convention for the THOR-50M time-histories. Table 9 shows the CORA scores for the belted THOR-50M driver. For the Half V0 tests, the average CORA scores for the driver in the Small, Mid-size, and Large PU vehicles were 0.866, 0.760, and 0.723, respectively. For the Half V1 tests, the average CORA scores for the driver in the Small and Large PU were 0.789 and 0.658, respectively.

For the Small vehicle, the Half V0 test showed relatively comparable results for the driver measurements, with all CORA scores in the “Good” or “Acceptable” range and the lowest CORA score being 0.720. In the Half V1 test, on the other hand, there were more “Acceptable” results and one “Poor” result. The “Poor” result occurred in the upper left tibia axial force measurement (TibiaLUFz), where the shape, phase, and magnitude of the Half V1 time-history appear qualitatively similar to the Half V0 and Full designs (Figure 36). However, quantitatively, the CORA component scores were below 0.58 for the corridor and shape components, resulting in an overall score of 0.572. For comparison, the upper right tibia axial force measurement (TibiaRUFz) in the Half V1 test showed a CORA score of 0.729, but was visually distinct from tests of the Half V0 and Full barrier designs (Figure 37).

Table 8
Naming convention for THOR-50M time-histories

Name	Description
HeadACRes	Head CG resultant acceleration
HeadAVx	Head CG angular velocity (x)
HeadAVy	Head CG angular velocity (y)
HeadAVz	Head CG angular velocity (z)
NeckFz	Upper neck force (z)
NeckMy	Upper neck moment (y)
ChestLL	Resultant left lower chest displacement
ChestRL	Resultant right lower chest displacement
ChestLU	Resultant left upper chest displacement
ChestRU	Resultant right upper chest displacement
AcetabRIRes	Resultant right acetabular force
AcetabLERes	Resultant left acetabular force
FemurLE	Left femur force (z)
FemurRI	Right femur force (z)
TibiaRUFz	Right upper tibia force (z)
TibiaRUMomRes	Right upper tibia moment resultant (x,y)
TibiaRLFz	Right lower tibia force (z)
TibiaRLMomRes	Right lower tibia moment resultant (x,y)
TibiaLUFz	Left upper tibia force (z)
TibiaLUMomRes	Left upper tibia moment resultant (x,y)
TibiaLLFz	Left lower tibia force (z)
TibiaLLMomRes	Left lower tibia moment resultant (x,y)

Table 9
CORA scores for belted driver THOR-50M response when the OMDB impacts production vehicles

	Small		Mid-size		Large PU	
	V0 ¹	V1	V0	V1 ²	V0	V1
HeadACRes	0.928	0.961	0.936	NA	0.888	0.826
HeadAVx	0.772	0.921	0.904	NA	0.652	0.629
HeadAVy	0.904	0.847	0.920	NA	0.714	0.787
HeadAVz	0.827	0.884	QD	NA	0.508	0.501
NeckFz	0.873	0.903	0.873	NA	0.851	0.331
NeckMy	0.799	0.661	0.657	NA	0.718	0.672
ChestLL	QD	QD	0.509	NA	0.750	0.637
ChestRL	0.926	0.948	0.535	NA	0.681	0.927
ChestLU	QD	QD	0.621	NA	0.826	0.586
ChestRU	0.936	0.919	0.621	NA	QD	QD
AcetabRIRes	0.928	0.741	0.907	NA	0.799	0.619
AcetabLERes	0.808	0.743	0.855	NA	0.908	0.622
FemurLE	0.813	0.763	0.470	NA	0.772	0.736
FemurRI	0.969	0.783	0.883	NA	0.627	0.601
TibiaRUFz	0.936	0.789	0.807	NA	0.673	0.662
TibiaRUMomRes	0.902	0.663	0.712	NA	0.735	0.748
TibiaRLFz	0.964	0.839	0.883	NA	0.585	0.663
TibiaRLMomRes	0.879	0.672	0.802	NA	0.807	0.863
TibiaLUFz	0.787	0.572	0.665	NA	0.290	0.361
TibiaLUMomRes	0.792	0.722	0.812	NA	0.890	0.702
TibiaLLFz	0.848	0.729	0.774	NA	QD	QD
TibiaLLMomRes	0.720	0.721	0.816	NA	0.793	0.677
Average	0.866	0.789	0.760	NA	0.723	0.658

QD – Questable data

NA – Not applicable, test was not performed for this vehicle

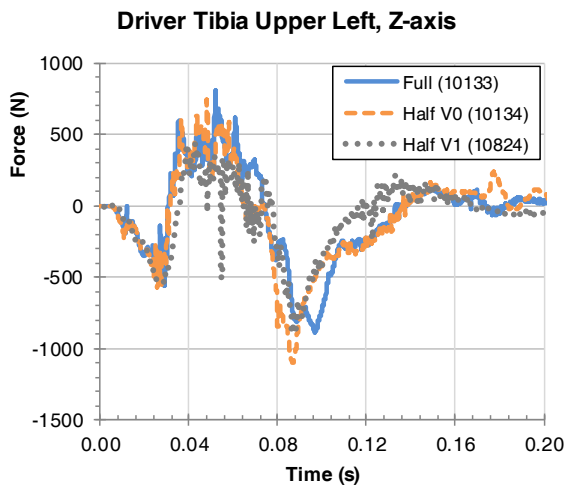


Figure 36 Driver left upper tibia Z-axis force for the Small vehicle in the Full, Half V0, and Half V1 conditions.

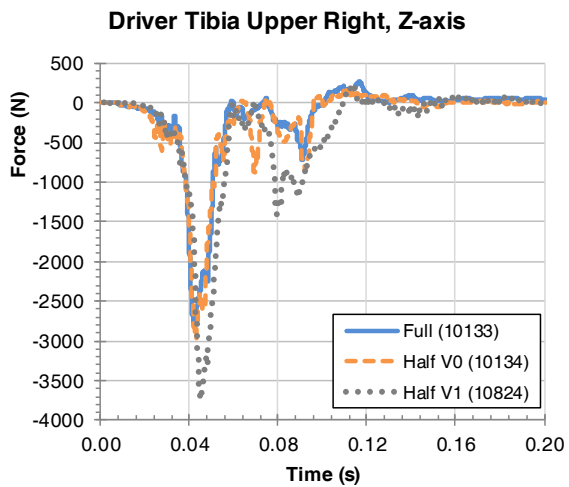


Figure 37 Driver right upper tibia Z-axis force for the Small vehicle in the Full, Half V0, and Half V1 conditions.

For the Mid-size vehicle, where only the Half V0 barrier test was conducted, CORA scores for the driver measurements were evenly split between “Good” and “Acceptable”, with three scores falling in the “Poor” range: ChestLL, ChestRL, and FemurLE. The lower left chest resultant deflection (ChestLL) was higher in the Full condition (Figure 38), while the lower right chest resultant deflection (ChestRL) was higher in the Half V0 condition (Figure 39). However, these differences are unlikely to have implications in injury risk prediction, as the peak resultant deflection occurred in the upper right chest in the Mid-size vehicle in both barrier conditions. That said, the overall peak resultant deflection was about 12 millimeters higher in the Half V0 condition, which is surprising since the shoulder belt force time-histories were nearly identical between the Full and Half V0 conditions, and the vehicle crash pulse in the Full condition was slightly more severe. One possible explanation is the initial position of the driver, which may have been further from the steering wheel airbag in the Full condition compared to the Half V0 condition as evidenced by pre-test position measurements at the chest to dash (Full: 596 mm, Half V0: 570 mm), chest to steering hub (Full: 377 mm, Half V0: 342 mm), and rim to abdomen (Full: 225 mm, Half V0: 197 mm) locations. Similarly, the left knee-to-dash distance was 10 mm greater in the Full condition, which may have reduced the magnitude of interaction of the knee with the knee bolster and subsequently reduced the left femur compressive force (FemurLE) compared to the Half V0 condition (Figure 40).

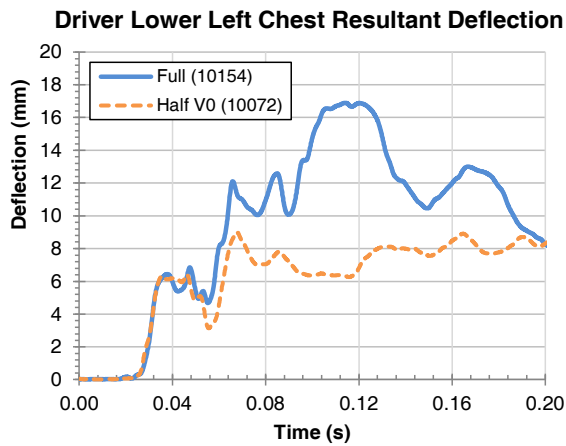


Figure 38 Driver lower left chest resultant deflection for the Mid-size vehicle in the Full and Half V0 conditions.

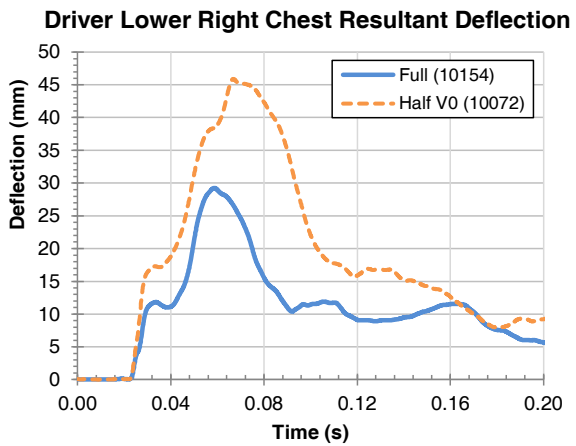


Figure 39 Driver lower right chest resultant deflection for the Mid-size vehicle in the Full and Half V0 conditions.

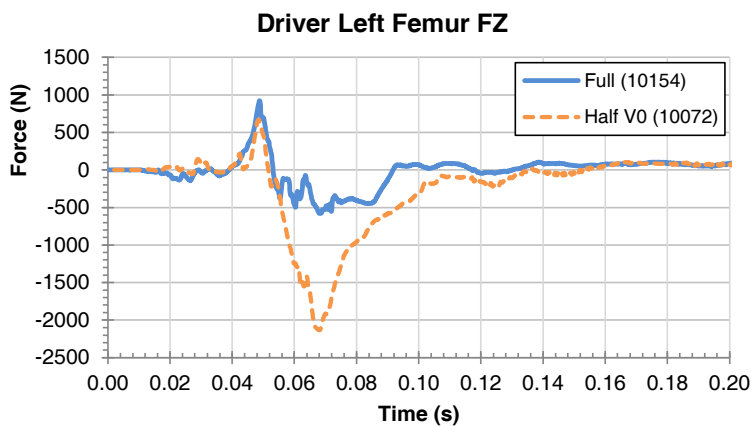


Figure 40 Driver left femur Z-axis force for the Mid-size vehicle in the Full and Half V0 conditions.

The Large PU tests showed more differences in driver response between the Full and the Half barrier tests than the other two production vehicles. In the Half V0 condition, there were 6 “Good” and 2 “Poor” scores, while in the Half V1 condition, there were 3 “Good” and 3 “Poor” scores, with the remainder falling into the “Average” range. The “Poor” scores for the Half V0 condition occurred in the HeadAVz and TibiaLUFz measurements. Differences in the head angular rate about the Z-axis are apparent across all three barrier conditions (Figure 41), as the Half V0 and Half V1 conditions show an early positive peak that does not occur in the Full test. Review of the high-speed video shows that, compared to the Full condition, the head contacts closer to the center of the steering wheel airbag in the Half V0 and Half V1 conditions, resulting in inboard rotation of the head. This difference does result in noticeable differences in the Brain Injury Criterion (BrIC) for the driver in the Large PU tests, as the BrIC in the Full barrier condition (0.66) was lower than in the Half V0 (0.89) and Half V1 (0.86) conditions. Differences in the left upper tibia axial force showed a similar trend, where the Half V0 and Half V1 responses were more similar to each other than to the Full barrier condition (Figure 42). However, the three conditions showed similar peak compressive forces, which were all relatively low both compared to risk of injury (probability of AIS 2+ injury below 1 percent) and compared to the peak tibia compressive forces in other tibia locations throughout the Large PU tests.

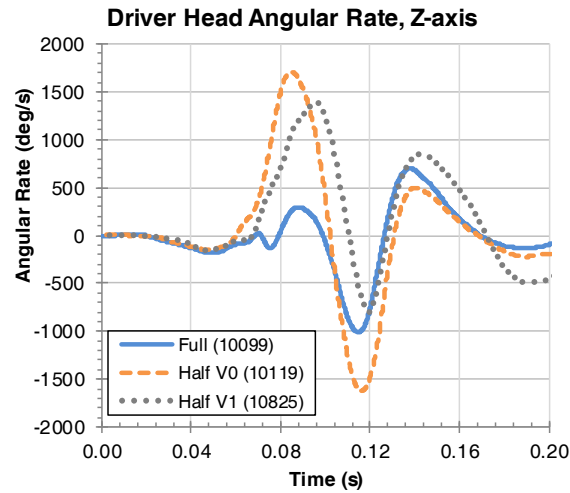


Figure 41 Driver Z-axis head angular rate for the Large PU in the Full, Half V0, and Half V1 conditions.

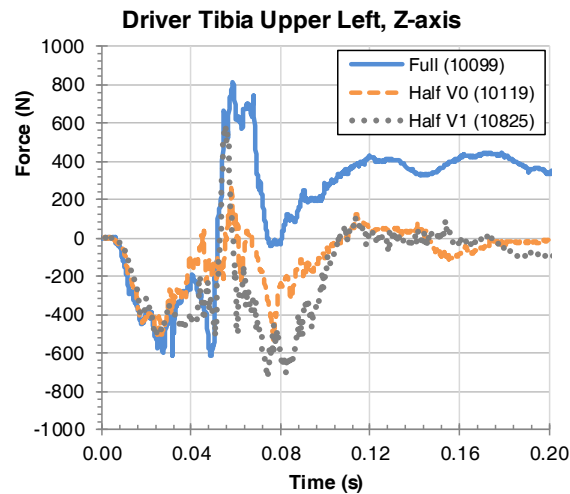


Figure 42 Driver left upper tibia Z-axis force for the Large PU in the Full, Half V0, and Half V1 conditions.

The “Poor” scores for the driver in the Large PU in the Half V1 condition also occurred in the HeadAVz, and TibiaLUFz measurements, as discussed above, but also the NeckFz measurements. The neck axial force time-history (NeckFz) in the Half V1 condition showed similar timing to the Full condition, but the peak tension is about 340 N lower than the Full and Half V0 conditions (Figure 43). Review of the high-speed video from these tests did not identify differences in head and neck kinematics, though the difference in neck tension may have resulted from the difference in vehicle crash pulse (Figure 33).

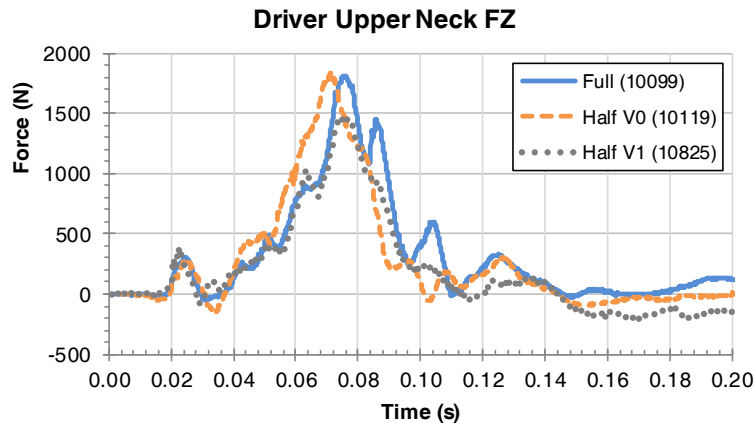


Figure 43 Driver upper neck Z-axis force for the Large PU in the Full, Half V0, and Half V1 conditions.

Occupant Response: Passenger

Within each production vehicle, right front passenger kinematics were similar across all barrier designs. Table 10 shows the CORA scores for the belted THOR-50M passenger. For the Half V0 tests, the average CORA ratings for the right front passenger in the Small, Mid-size, and Large PU vehicles were all in the “Good” range, with scores of 0.867, 0.852, and 0.842, respectively. For the Half V1 tests, the average CORA ratings for the right front passenger in the Small and Large PU were “Acceptable”, with scores of 0.762 and 0.689, respectively.

For the Small vehicle, the Half V0 test showed relatively comparable results for the right front passenger measurements, with all CORA scores in the “Good” or “Acceptable” range, with a lowest CORA score of 0.706. In the Half V1 test, on the other hand, there were more “Acceptable” results and two “Poor” results. One of the “Poor” results was the neck moment (NeckMy), where the Half V1 test showed a similar response to the other two conditions except for between 110 and 160 ms, where the extension moment was lower (Figure 44). While there were differences in the resulting Nij values (Full: 0.38, Half V0: 0.37, Half V1: 0.45), the elevated Nij in the Half V1 condition appears to result from a higher peak in neck axial force (NeckFZ) at roughly 80 ms after impact. The other “Poor” result occurred in the upper right tibia resultant moment measurement (TibiaRUMomRes), where the Half V1 condition showed a different response trend, with lower moments up to 50 ms and higher moments between 50 and 100 ms after impact (Figure 46). The upper left tibia resultant moment (TibiaLUMomRes), which also had a relatively low CORA score at 0.589, showed the opposite trend, with higher moments earlier and lower moments later in the event (Figure 45).

Table 10
CORA scores for belted passenger THOR-50M response when the OMDB impacts production vehicles

	Small		Mid-size		Large PU	
	V0 ¹	V1	V0	V1 ²	V0	V1
HeadACRes	QD	QD	0.892	NA	0.971	0.899
HeadAVx	0.740	0.926	0.824	NA	0.955	0.913
HeadAVy	0.873	0.763	0.880	NA	0.910	0.901
HeadAVz	0.921	0.868	QD	NA	0.919	0.853
NeckFz	0.732	0.830	0.801	NA	0.792	0.739
NeckMy	0.873	0.476	0.783	NA	0.776	0.312
ChestLL	0.956	0.730	0.878	NA	0.862	0.804
ChestRL	0.837	0.758	0.711	NA	0.846	0.565
ChestLU	0.930	0.799	0.915	NA	QD	QD
ChestRU	0.706	0.661	0.830	NA	0.719	0.627
AcetabRIRes	QD	QD	0.885	NA	0.783	QD
AcetabLERes	0.839	0.878	QD	NA	0.718	0.539
FemurLE	0.972	0.843	0.890	NA	0.940	0.830
FemurRI	0.929	0.747	0.890	NA	0.928	0.917
TibiaRUFz	0.952	0.808	0.885	NA	0.842	0.654
TibiaRUMomRes	0.877	0.538	0.708	NA	0.864	0.570
TibiaRLFz	0.964	0.827	0.925	NA	0.849	0.577
TibiaRLMomRes	0.792	0.638	0.916	NA	0.849	0.400
TibiaLUFz	0.928	0.877	0.904	NA	0.725	0.597
TibiaLUMomRes	0.754	0.589	0.708	NA	0.838	0.722
TibiaLLFz	0.928	0.864	0.900	NA	QD	QD
TibiaLLMomRes	0.840	0.812	0.912	NA	0.756	0.678
Average	0.867	0.762	0.852	NA	0.842	0.689

QD – Questable data

NA – Not applicable, test was not performed for this vehicle

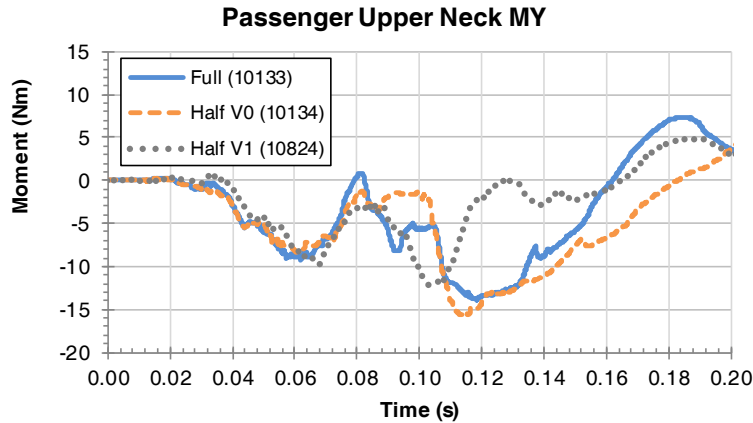


Figure 44 Passenger upper neck Y-axis moment for the Small vehicle in the Full, Half V0, and Half V1 conditions.

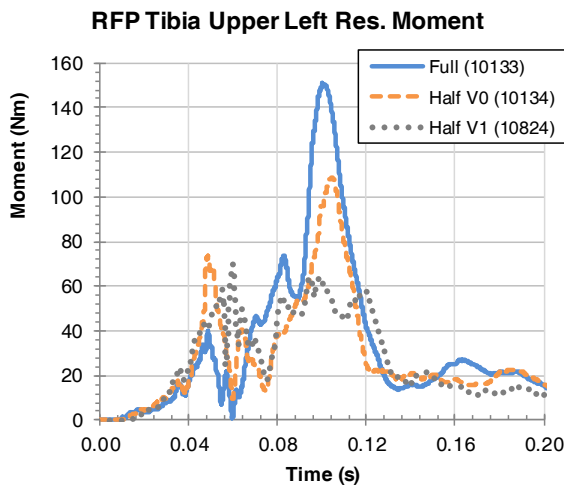


Figure 45 Passenger upper left tibia resultant moment for the Small vehicle in the Full, Half V0, and Half V1 conditions.

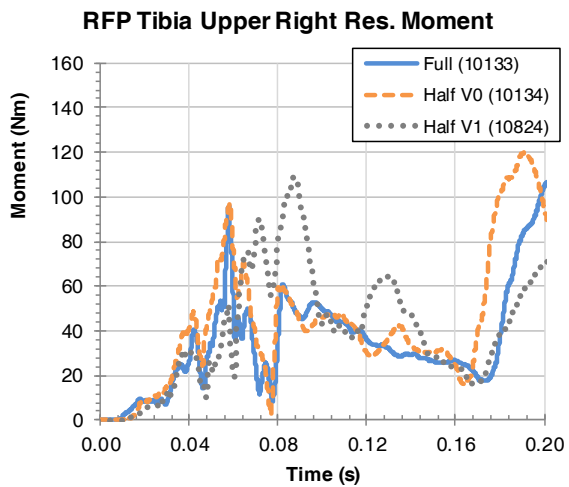


Figure 46 Passenger upper right tibia resultant moment for the Small vehicle in the Full, Half V0, and Half V1 conditions.

The passenger measurements in the Half V0 test of the Mid-size vehicle showed relatively comparable results, with all CORA scores in the “Good” or “Acceptable” range and the minimum CORA score being 0.708. The Half V0 results for the right front passenger in the Large PU were similar, with a few more measurements falling in the “Acceptable” range but with all scores at or above 0.718.

The right front passenger measurements in the Half V1 test of the Large PU, on the other hand, were evenly divided between “Good” (7 measurements), “Acceptable” (7 measurements), and “Poor” (6 measurements). The “Poor” measurements were NeckMy, ChestRL, AcetabLERes, TibiaRUMomRes, TibiaRLFz, and TibiaRLMomRes. As with previous “Poor” assessments of NeckMy, the resulting Nij injury criteria calculation does not appear to be influenced by the variation of the neck Y-axis moment (Full: 0.30; Half V0: 0.27; Half V1: 0.31). Similarly, the variation in the lower right chest resultant deflection (ChestRL) does not influence injury prediction, as the peak resultant deflection occurs in either the upper left or upper right quadrants of the right front passenger in the Large PU tests. The variation in the left acetabulum resultant force (AcetabLERes) occurs primarily after the peak femur force occurs (Figure 47), thus the second peaks that occur after 100 ms in the Half V0 and Half V1 tests (Figure 48) do not contribute to acetabulum injury risk. In both the femur and acetabulum force time-histories, the largest magnitude of force occurs in the Full condition, followed by the Half V0 and then the Half V1 conditions. This is

consistent with the vehicle crash pulses shown in Figure 32 and Figure 33, which suggest that the Half V1 condition presented the least severe pulse to the occupants. Similarly, in the lower leg of the right front passenger of the Large PU, the right upper tibia resultant moment (TibiaRUMomRes), right lower tibia Z-axis force (TibiaRLFz), and right lower tibia resultant moment (TibiaRLMomRes) all demonstrate forces that are generally lower for the Half V1 than the Half V0 and Full conditions (Figure 50 through 52).

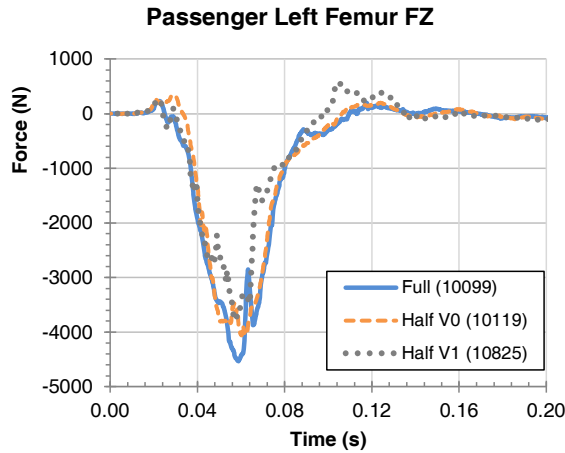


Figure 47 Passenger left femur Z-axis force for the Large PU vehicle in the Full, Half V0, and Half V1 conditions.

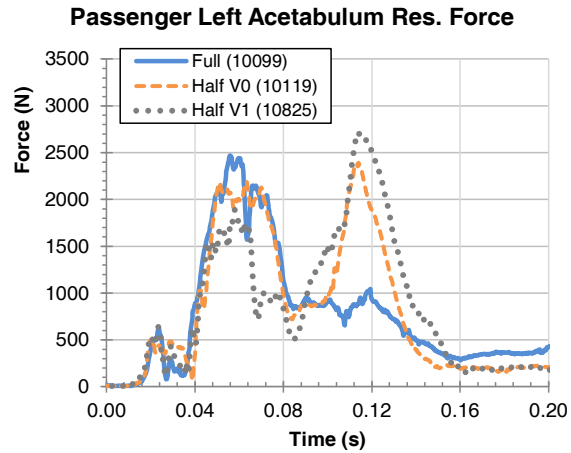


Figure 48 Passenger left acetabulum resultant force for the Large PU vehicle in the Full, Half V0, and Half V1 conditions.

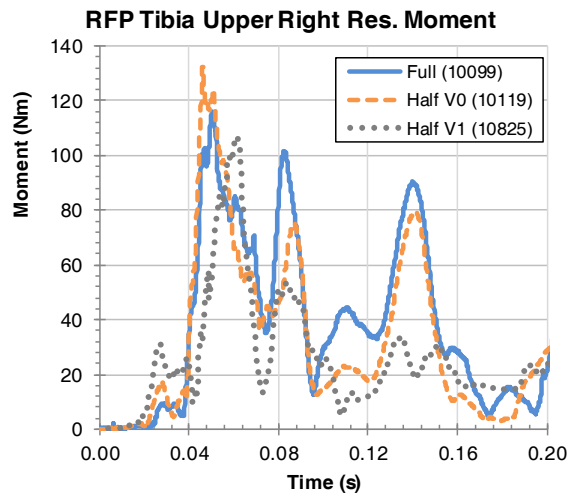


Figure 49 Passenger upper right tibia resultant moment for the Large PU vehicle in the Full, Half V0, and Half V1 conditions.

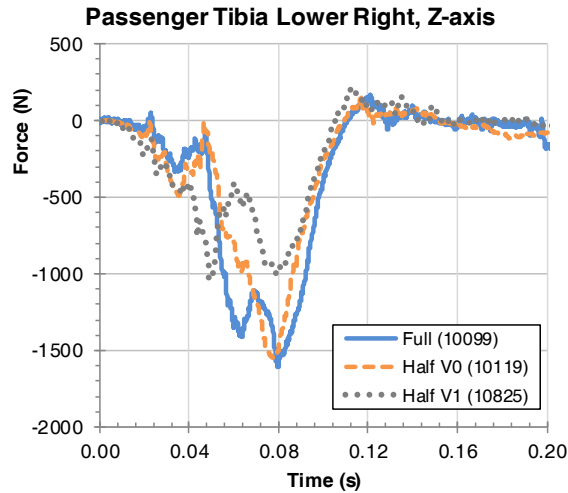


Figure 50 Passenger lower right tibia Z-axis force for the Large PU vehicle in the Full, Half V0, and Half V1 conditions.

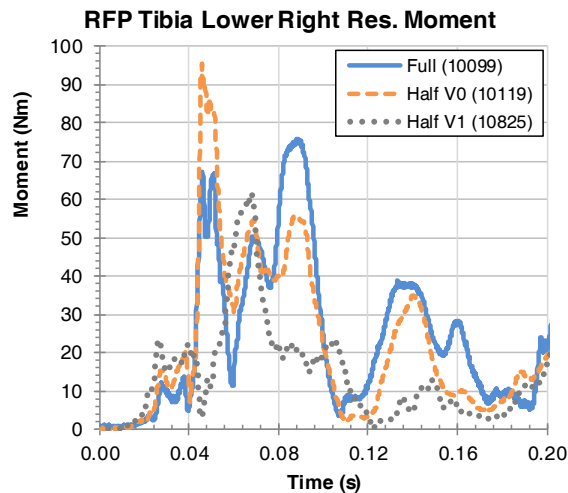


Figure 51 Passenger lower right tibia resultant moment for the Large PU vehicle in the Full, Half V0, and Half V1 conditions

Rigid Moving Barrier Response

Half V0 seems to be a suitable replacement of the Full barrier. Therefore, a set of tests were performed using a rigid moving barrier instead of production vehicles to eliminate variability in response of production vehicles. Using this rigid barrier eliminates the variability of vehicle deformation. The rigid moving barrier used for this testing was an FMVSS No. 301 Moving Contoured Barrier (MCB) (Figure 52).

Six tests were performed with alternating installation of full and half honeycomb barriers (Table 11). The first test was performed at an impact speed of 70 km/h with a full honeycomb barrier installed on the OMDB. The energy of the OMDB impact caused some of the MCB's face plate fasteners to fail and resulted in minor deformations to the MCB supporting structure. The MCB was repaired and strengthened to prevent deformation in further testing. This led to an increase in the MCB weight of approximately 92 kg, resulting in a final weight of 1,898 kg, without a significant change in the fore/aft location (< 8 mm) of the vehicle center of gravity (CG).

For the remaining five tests, the impact speed of the OMDB was reduced to 60 km/h. A total of three half honeycomb barrier and two full honeycomb barrier tests were run at this test speed. Tests using the half honeycomb barrier mounted it on the left side of the OMDB.

Table 11
Test matrix for MDB testing

NHTSA Test Number	Barrier Type	Naming Convention
9796	Full	NA *
9797	Full	Full 1
9799	Full	Full 2
9796	Half V0	Half V0 1
9798	Half V0	Half V0 2
9800	Half V0	Half V0 3

* NA – Not applicable, test caused damage to cart



Figure 52 Picture of the moving contoured barrier (MCB)

Figure 53 shows the energy absorbed by the honeycomb when impacting the MCB. It is seen that the average energy absorbed by the honeycomb Half V0 is decreased by 15 percent when compared to Full.

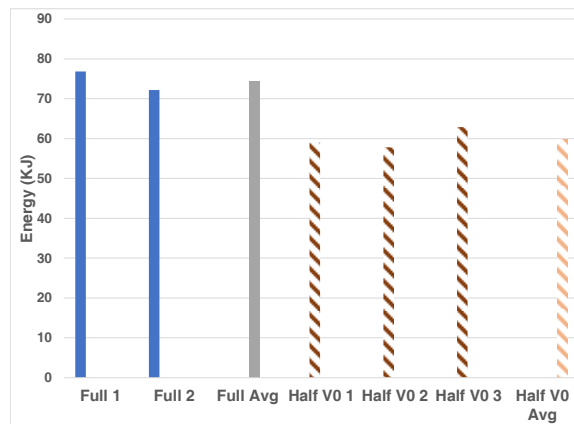


Figure 53 Energy absorbed by the honeycomb when the OMDB impacts the MCB

Figure 54 through Figure 56 show the crush profiles, for different rows, for the Full and Half V0 when impacting the MCB. It is seen that the crush profile of Half V0 is shifted to the right when compared to Full. R3 had more variability in crush compared to R6 and R9.

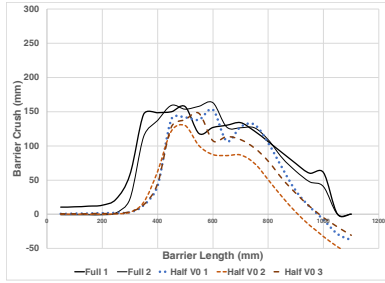


Figure 54 R3 honeycomb crush when impacting MCB

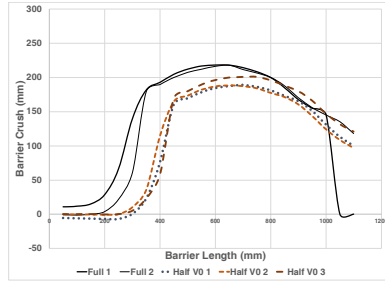


Figure 55 R6 honeycomb crush when impacting MCB

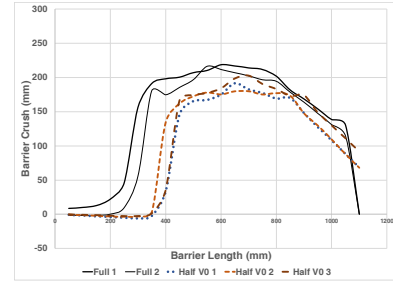


Figure 56 R9 honeycomb crush when impacting MCB

Table 12 shows the naming convention for MCB time-histories when using MCB as a target vehicle. Table 13 shows the naming convention for the OMDB when using the MCB as a target vehicle.

Table 14 shows the CORA scores for the OMDB when impacting the MCB. It is seen that the lowest CORA score is for the OMDBMCBCGav (0.902) and the average CORA score for all OMDB parameters was 0.947. Table 15 shows the CORA scores for the MCB responses. It can be seen from this table that the CORA scores ranged from 0.424 to 0.997 and the average CORA score was 0.807. The MCBCGav and MCBCGang were graded “poor.” To investigate why the CORA scores were “Poor”, film analysis was performed on the MCB. Figure 57 shows the time-histories for the MCB rotation. The figure shows differences between each test, but film analysis showed closer similarity of the rotation (Figure 59). Running CORA on the film analysis increased the CORA score to Acceptable (0.789). It is unknown why the integration of the angular velocity showed different results than the film analysis.

Table 12
Naming convention for MCB time-histories when using MCB as target vehicle

Name	Description
MCBCGaccRes	MCB CG resultant acceleration (x,y)
MCBCGvelRes	MCB CG resultant velocity (x,y)
MCBCGav	MCB CG angular velocity (z)
MCBCGang	MCB CG rotation (z)
MCBRearAccRes	MCB centerline rear resultant acceleration (x,y)
MCBRearVelRes	MCB centerline rear resultant velocity (x,y)
MCBLeftAccRes	MCB left frame resultant acceleration (x,y)
MCBLeftVelRes	MCB left frame resultant velocity (x,y)

Table 13
Naming convention for OMDB time-histories when using MCB as target vehicle

Name	Description
OMDBMCBCGaccRes	OMDB CG resultant acceleration (x,y)
OMDBMCBCGvelRes	OMDB CG resultant velocity (x,y)
OMDBMCBCGav	OMDB CG angular velocity (z)
OMDBMCBCGang	OMDB CG rotation (z)*
OMDBMCBRearAccRes	OMDB centerline rear resultant acceleration (x,y)
OMDBMCBRearVelRes	OMDB centerline rear resultant velocity (x,y)
OMDBMCBLeftAccRes	OMDB left frame resultant acceleration (x,y)
OMDBMCBLeftVelRes	OMDB left frame resultant velocity (x,y)*

Table 14
CORA scores for the OMDB when the OMDB impacts the MCB

Name	CORA	Name	CORA
OMDBMCBCGaccRes	0.869	OMDBMCBRearAccRes	0.943
OMDBMCBCGvelRes	0.965	OMDBMCBRearVelRes	0.989
OMDBMCBCGav	0.902	OMDBMCBLeftAccRes	0.952
OMDBMCBCGang	0.972	OMDBMCBLeftVelRes	0.987
		Average of all scores	0.947

Table 15
CORA scores for the MCB when the OMDB impacts the MCB

Name	CORA	Name	CORA
MCBCGaccRes	0.887	MCBRearAccRes	0.820
MCBCGvelRes	0.954	MCBRearVelRes	0.908
MCBCGav	0.424	MCBLeftAccRes	0.967
MCBCGang	0.497	MCBLeftVelRes	0.997
		Average of all scores	0.807

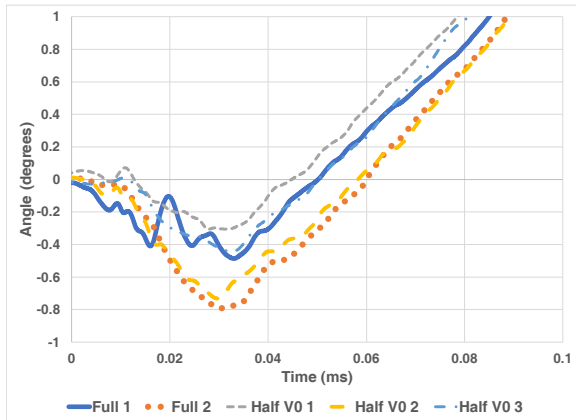


Figure 57 MCB rotation about the z-axis time-histories

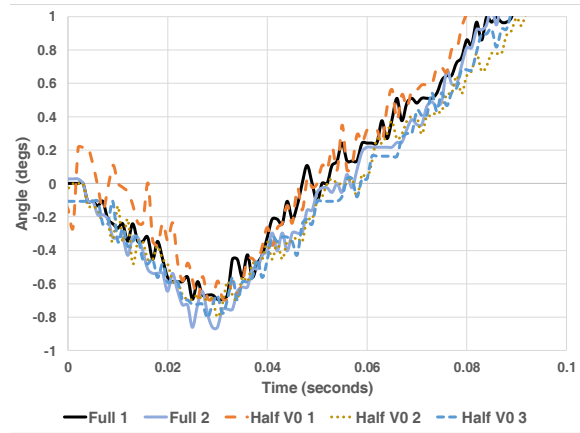


Figure 58 MCB rotation about the z-axis from film analysis

DISCUSSION

OMDB, Vehicle

Attaching the left side of the honeycomb to the OMDB attachment (Half V1) prevented the honeycomb from expanding out from the OMDB (Figure 59), but it did not prevent all barrier separation. Figure 60 shows an example of the honeycomb separation with the small vehicle when impacted with the Half V1. Again, it is unknown what effect this separation has on the performance of this test procedure. A side effect of attaching the medial end of the cladding to the barrier support in the Half V1 design was that it changed the magnitude of energy absorbed by the honeycomb (Figure 8). This was especially true for the Large PU, where the energy absorbed in the Half V1 design was 32 percent lower than in the Full design. Similarly, the interior intrusions differed in the Half V1 design compared to the other barrier faces, especially for the Large PU (Figure 31). The Half V1 also showed a difference in acceleration.



Figure 59 No honeycomb pulling apart from the Half V1

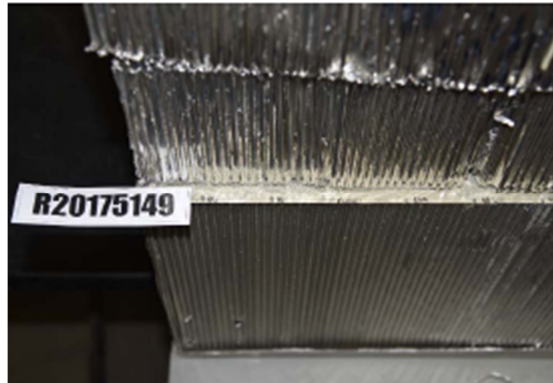


Figure 60 Separation of the two pieces of honeycomb for the Half V1 when impacting the small vehicle

Occupant Response

Overall, the occupant kinematics in tests of different barrier designs using the same production vehicle were similar, as evidenced by review of the high-speed video from cameras mounted within the vehicle looking over the inboard shoulder of the occupant. Contacts with the restraint system occurred at similar times and locations, with the exception of the driver contact with the steering wheel airbag in the Large PU tests, where the head impacted closer to the center of the airbag in the Full test than tests of the Half V0 and Half V1 designs. This visible difference in head kinematics was captured by the head injury criteria, as the HIC and BrIC metrics in the Full condition were 10 percent and 25 percent lower, respectively, than in the Half V0 and Half V1 conditions. Otherwise, many of the differences in occupant kinetics time-histories occurred in the femur and upper tibia, areas which were not readily visible in these camera views due to interference from frontal airbags and the torso of the occupant.

In the Small and Large PU OMDB tests, the Half V0 barrier face showed higher CORA scores for occupant response than the Half V1 barrier, suggesting that the Half V0 performance is more similar to the Full barrier face than the Half V1 design. While there was no data available to compare Half V0 and Half V1 in the Mid-size vehicle, the average CORA scores for the Half V0 were similar to those in the Small and Large PU vehicles. In a previous study of the repeatability and reproducibility of the OMDB test procedure, average CORA scores across three tests using the same Full barrier face in impacts with a production sport-utility vehicle ranged from 0.772 to 0.850 depending on the test lab conducting the tests [3]. Therefore, based on objective evaluation of occupant response time-histories, the difference between the Half V0 barrier face and the Full barrier face is within the range of expected test-to-test repeatability of the Full barrier face itself.

The driver occupant location appeared to be more sensitive to changes in the barrier face, as the average CORA scores for each vehicle/barrier comparison were equal or lower for the driver than for the right front passenger. One possible explanation for this finding is that the driver side of the occupant compartment sees more intrusion, both static and dynamic, than the passenger side due to the configuration of the crash test (Figure 6). Measured static intrusions, as shown in Figure 29 through Figure 31, varied between the different barrier face conditions; dynamic

intrusion is more difficult to quantify, but can be seen in the high-speed video. In contrast, the passenger side of the occupant compartment sees little to no intrusion, presenting more consistent boundary conditions to the right front passenger.

In some of the test conditions, the same THOR-50M ATD was used for all two or three tests in a given seating location, while others used a different THOR-50M ATD in the Half V1 test condition (Table 16). For example, the driver in the Large PU was serial number (S/N) 9798 for all three barrier conditions, while the right front passenger was S/N 9207 in the Full and Half V0 conditions, but EG2595 in the Half V1 condition. In theory, this data could be used to assess the repeatability and reproducibility of the THOR-50M, though in practice the variation in barrier face and vehicle response prevented a clean comparison. As an example, since the same THOR-50M ATD was used in the driver location of the Large PU tests, the variability was expected to be the smallest. However, the average CORA scores for both the Half V0 and Half V1 conditions were actually the lowest out of all vehicles and seating positions in the study. Therefore, it is not possible to separate the variability in the ATD response from the variability in the barrier and/or vehicle response. On the other hand, the fact that the tests using EG2595, which included an onboard data acquisition system (DAS), had average CORA scores equal to or higher than the driver ATD in the same vehicle/barrier condition suggests that the differences in response were not driven by the differences between an onboard DAS system and an umbilical configuration.

Table 16. Occupant response repeatability and reproducibility

TSTNO	Vehicle Class	Barrier Face	Driver S/N	Driver Average CORA Score	RFP S/N	RFP Average CORA Score
10099	Small	Full	9207		9798	
10119		Half V0	9207	0.866	9798	0.867
10825		Half V1	9798	0.789	EG2595	0.762
10154	Mid-size	Full	9798		9207	
10072		Half V0	9798	0.760	9207	0.852
10133	Large PU	Full	9798		9207	
10134		Half V0	9798	0.723	9207	0.842
10824		Half V1	9798	0.658	EG2595	0.689

CONCLUSIONS

This study evaluated the performance of two half-width barrier faces compared to a full-width barrier face in OMDB crash tests of three classes of production vehicles. This analysis compared the responses of the barriers, vehicles, and occupants using an objective evaluation method. Based on this objective evaluation using CORA scores, the Half V0 barrier face design was more similar to the Full barrier face than the Half V1 design. The Half V0 demonstrated average CORA scores in the “Good” category for the OMDB and vehicle measurements in tests of all three production vehicles, and average occupant response measurements in the “Good” category for 4 of the 6 occupant locations, and higher CORA scores than the Half V1 barrier in all cases. The Half V0 barrier design did result in post-test separation of the two layers of honeycomb in the design, but it’s not clear how this differs from the Full barrier design. It is also not clear what the consequences of this separation might be, though one possible challenge would be representing this separation in computational models of this barrier face. It was clear, however, that attempts to prevent this separation in the Half V1 design resulted in differences in the barrier face crush, vehicle intrusion, and occupant response compared to the Full barrier. Given these findings, the Half V0 barrier face design appears to be a reasonable alternative to the Full barrier face design for use in OMDB crash tests.

REFERENCES

- [1] [OMDB | NHTSA](#) NHTSA Frontal Mobile Deformable Half Barrier Face V2015b.
- [2] [OMDB | NHTSA](#) OMDB Frontal Mobile Deformable Barrier Face v2014.
- [3] Saunders, J. and Parent, D., “Repeatability and Reproducibility of Oblique Moving Deformable Barrier Test Procedure,” SAE Technical Paper 2018-01-1055, 2018, doi:10.4271/2018-01-1055.
- [4] <https://www.nhtsa.gov/research-data/research-testing-databases#/vehicle>.
- [5] National Highway Traffic Safety Administration, “Oblique Test Procedure,” Docket ID 2015-0119, 2016.
- [6] “CORApplus 4.0.4 (release date 2017-06-21),” [Online]. Available: <http://www.pdb-org.com/en/information/18-coradownload.html>.

APPENDIX A

**National Highway Traffic Safety Administration
(NHTSA)**

Oblique Mobile Deformable Half Barrier Face Specification

Version 2 (2019)

Table of Contents

1.0	INTRODUCTION.....	3
2.0	BARRIER COMPONENTS.....	4
3.0	MATERIAL SPECIFICATIONS & OVERALL DIMENSIONS	7
3.1	REAR HONEYCOMB BLOCK.....	7
3.2	FRONT HONEYCOMB BLOCK	7
3.3	BACKING SHEET.....	7
3.4	INTERMEDIATE SHEET.....	7
3.5	CONTACT SHEET	8
3.6	CLADDING SHEET	8
3.7	SIDE CLADDING	8
3.8	FRONT BRACKET.....	8
3.9	ADHESIVE.....	8
4.0	ADHESIVE BONDING PROCEDURE.....	9
5.0	ASSEMBLY PROCESS.....	10
5.1	BONDING HONEYCOMB TO ALUMINUM SHEETS	10
5.2	MOUNTING HOLES AND SLOTS.....	12
6.0	ASSEMBLY AND COMPONENT DRAWINGS	13

1.0 INTRODUCTION

The NHTSA Oblique Mobile Deformable Half Barrier Face V2019 is a 1200mm wide assembly of two layers of deformable aluminum honeycomb core. Each deformable core is 300 mm thick in the impact direction and is designed to provide a constant load in depth. The cores are adhesively bonded together with different aluminum sheets forming a ready to use deformable barrier to be fixed on a moving cart.

2.0 BARRIER COMPONENTS

The components of the barrier face are listed below and shown in Figure 1. The bonded surfaces are shown in Figure 2. The dimensions of the individual components of the barrier are listed in Section 3, with drawings found in Section 6.

1. Rear honeycomb block
2. Front honeycomb block
3. Backing sheet
4. Intermediate sheet
5. Contact sheet
6. Cladding sheet
7. Side bracket
8. Side cladding
9. Adhesive (Not Shown)

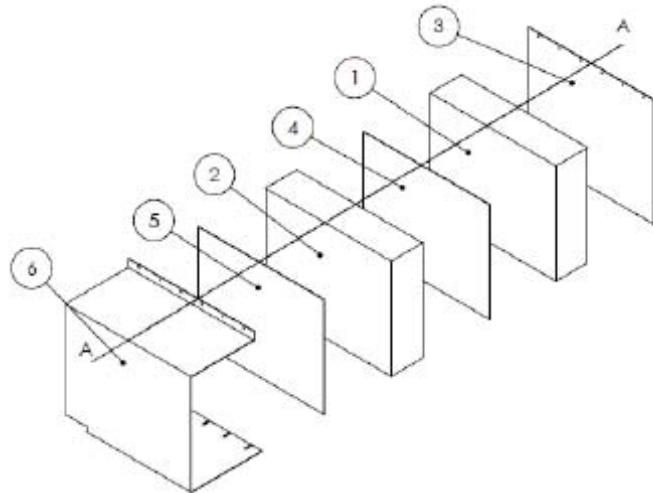


Figure 1 Components of Half Width Oblique Barrier (Core Body)

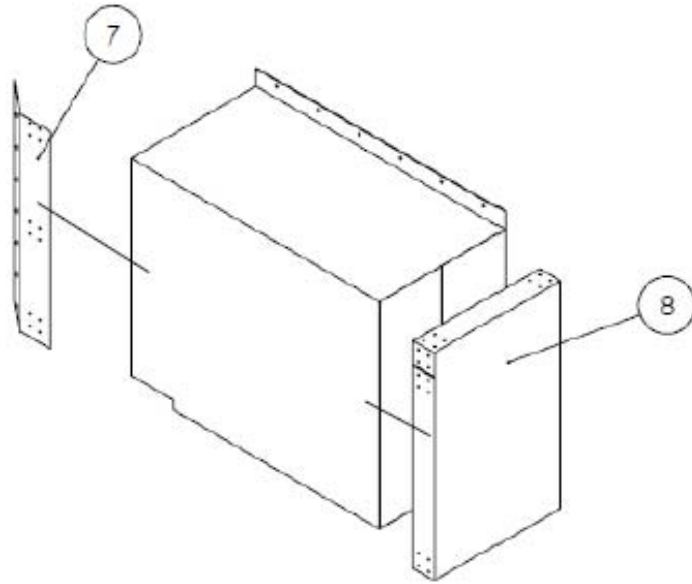
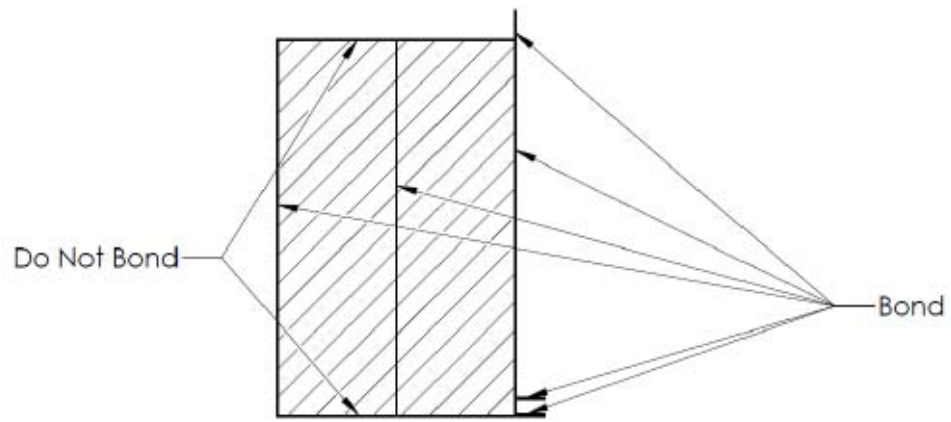


Figure 2 Components of Half Width Oblique Barrier (Core Body with Side Cladding and Side Bracket)



SECTION A-A

Figure 3 Cross-Section A-A – Adhesive Bonding of the Barrier

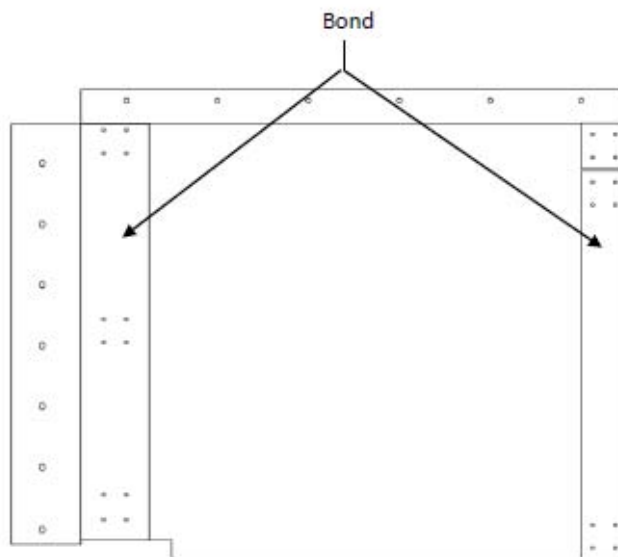


Figure 4 Front view – Adhesive Bonding of the Barrier continued

3.0 MATERIAL SPECIFICATIONS & OVERALL DIMENSIONS

3.1 REAR HONEYCOMB BLOCK

Dimensions:

Height (L): 950 ± 5 mm (in direction of honeycomb ribbon)
Width (W): 1200 ± 5 mm
Depth (T): 300 ± 1 mm (in direction of honeycomb cell)
Material: Aluminum 3003
Cell Size: 6.35 mm ± 20 percent
Crush Strength: 1.711 MPa +0 percent -10 percent¹

3.2 FRONT HONEYCOMB BLOCK

Dimensions:

Height (L): 950 ± 5 mm (in direction of honeycomb ribbon)
Width (W): 1200 ± 5 mm
Depth (T): 300 ± 1 mm (in direction of honeycomb cell)
Material: Aluminum 5052
Cell Size: 6.35 mm ± 20 percent
Crush Strength: 0.724 MPa +0 percent -10 percent¹

3.3 BACKING SHEET

Dimensions:

Height: 1025 mm ± 2.5 mm
Width: 1200 mm ± 2.5 mm
Thickness: 3.0 mm ± 0.25 mm
Material: Aluminum Series AlMg2 to AlMg3 with hardness between 50 and 67 HBS

3.4 INTERMEDIATE SHEET

Dimensions:

Height: 945 mm ± 2.5 mm
Width: 1195 mm ± 2.5 mm
Thickness: 0.5 ± 0.1 mm
Material: Aluminum 5251 H24 or Aluminum 5052 H32

¹In accordance with the certification procedure described in US Department of Transportation, NHTSA Laboratory Test Procedure for FMVSS No. 214 "Dynamic" Side Impact Protection, TP214D Appendix C Latest Revision.

3.5 CONTACT SHEET

Dimensions:

Height:	945 mm ± 2.5 mm
Width:	1195 mm ± 2.5 mm
Thickness:	1.6 mm ± 0.07 mm
Material:	Aluminum 5251 H24 or 5052 H34

3.6 CLADDING SHEET

Dimensions:

Height:	1026 mm ± 2.5 mm
Width:	1200 mm ± 2.5 mm
Thickness:	0.8 mm ± 0.1 mm
Material:	Aluminum 5754 H22 or 5052 H34

3.7 SIDE CLADDING

Dimensions:

Height:	952.5 mm ± 2.5 mm
Width:	601.75 mm ± 2.5 mm
Depth:	101 mm +/-2.5 mm
Thickness:	0.81 mm ± 0.1 mm
Material:	Aluminum 5754 H22 or 5052 H34

3.8 FRONT BRACKET

Dimensions:

Height:	918.5 mm ± 2.5 mm
Thickness:	0.81 mm ± 0.1 mm
Material:	Aluminum 5754 H22 or 5052 H34

3.9 ADHESIVE

The adhesive to be used throughout should be a Polyurethane adhesive or equivalent, with a minimum bonding strength of 0.6 MPa.²

² In accordance with the certification procedure described in ASTM C 297, using a sample of honeycomb representative of that in the impactor, bonded to a back plate material.

4.0 ADHESIVE BONDING PROCEDURE

Prior to bonding, all aluminum sheets shall be cleaned and prepared to provide optimal adhesion performance. The adhesive is only applied to the aluminum sheet surfaces when bonding aluminum sheets to honeycomb surfaces.

When bonding the cladding sheet to the backing sheet and when bonding the contact sheet to the cladding sheet, the adhesive is applied to one surface only.

A maximum of 0.5 kg/m² must be applied evenly over the surface, giving a maximum film thickness of 0.5 mm. Care should be taken to assure adhesive does not run into the honeycomb cells causing an increase in crushing strength of the honeycomb core.

5.0 ASSEMBLY PROCESS

5.1 BONDING HONEYCOMB TO ALUMINUM SHEETS

Verify that all surfaces are clean and prepared for bonding. The main part of the barrier face shall be assembled according to Figure 1. The rear honeycomb block shall be adhesively bonded to the backing sheet such that the cell axes are perpendicular to the backing sheet. The intermediate sheet shall be adhesively bonded to the rear and front honeycomb blocks. The cell axes of the front honeycomb block shall be perpendicular to the intermediate sheet. The contact sheet shall be adhesively bonded to the front honeycomb block. The outer cladding shall be adhesively bonded to the contact sheet. The top and bottom surfaces of the cladding sheet shall not be adhesively bonded to the main honeycomb block but should be positioned closely to it. The cladding sheet shall be adhesively bonded to the backing sheet at the mounting flanges. Side cladding will be adhesively bonded and riveted to the main body of the barrier. Likewise, the Front Bracket will be adhesively bonded, and riveted to the front of the main barrier body. All Rivets (32 in total) shall be ¼" aluminum button head Rivets. Bonding points can be seen in Figure 5 and Figure 6.

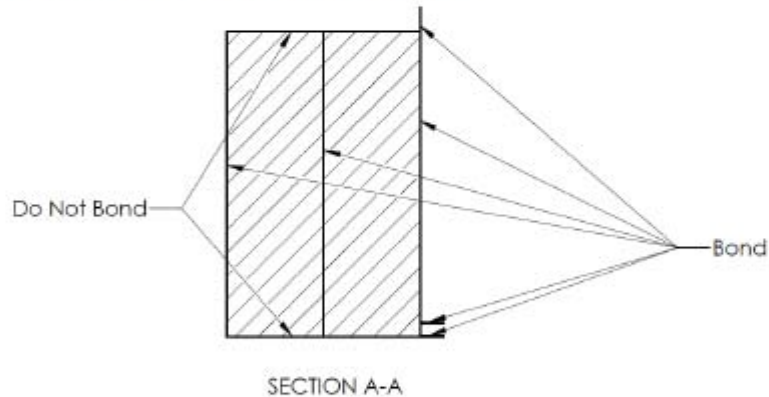


Figure 5 Main Body Assembly of the Barrier

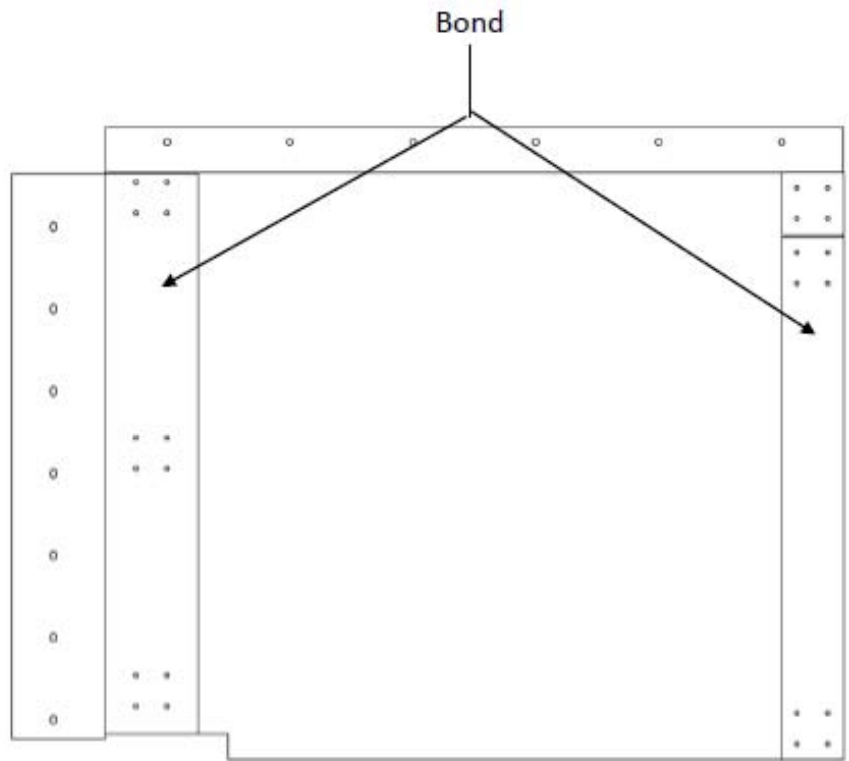


Figure 6 Main Body Assembly of the Barrier

5.2 MOUNTING HOLES AND SLOTS

The NHTSA Oblique Mobile Deformable Half Barrier V2019 has clearance holes and slots for mounting of the barrier. The holes shall have a diameter of 10.5mm. Six holes shall be located in the top flange at a nominal distance of 24.3mm from the top edge of the flange and six open slots in the bottom flange ending at a nominal distance of 60.2mm from the bottom edge of that flange. The holes and slots shall be at the locations shown in Figures 4 and 5. All holes and slots shall be located to ± 1 mm of the nominal distances.

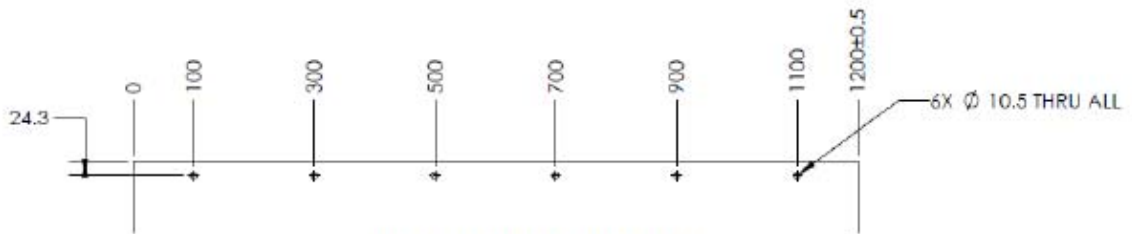


Figure 4 Top Flange Mounting Holes

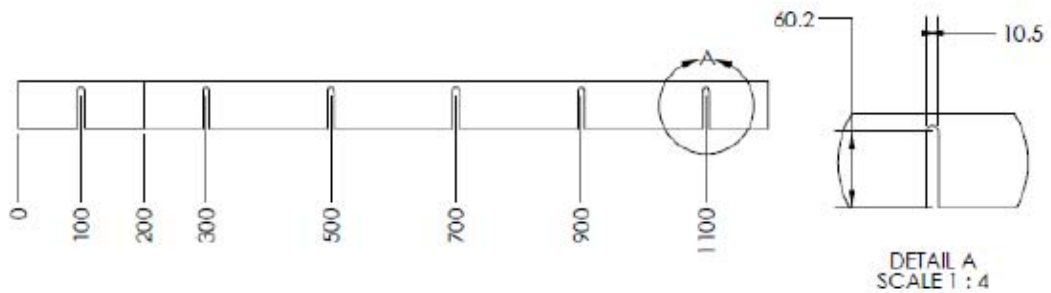
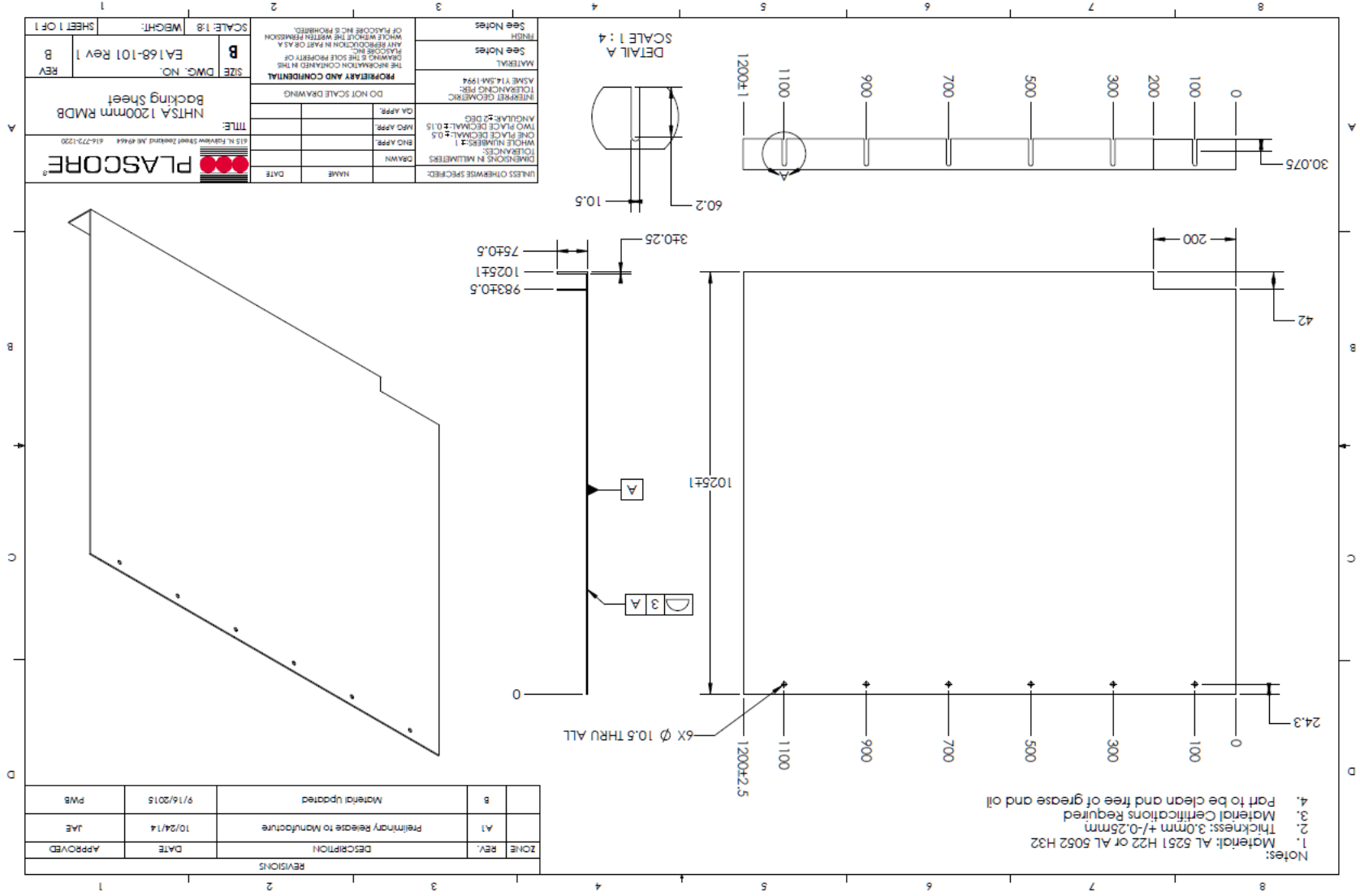
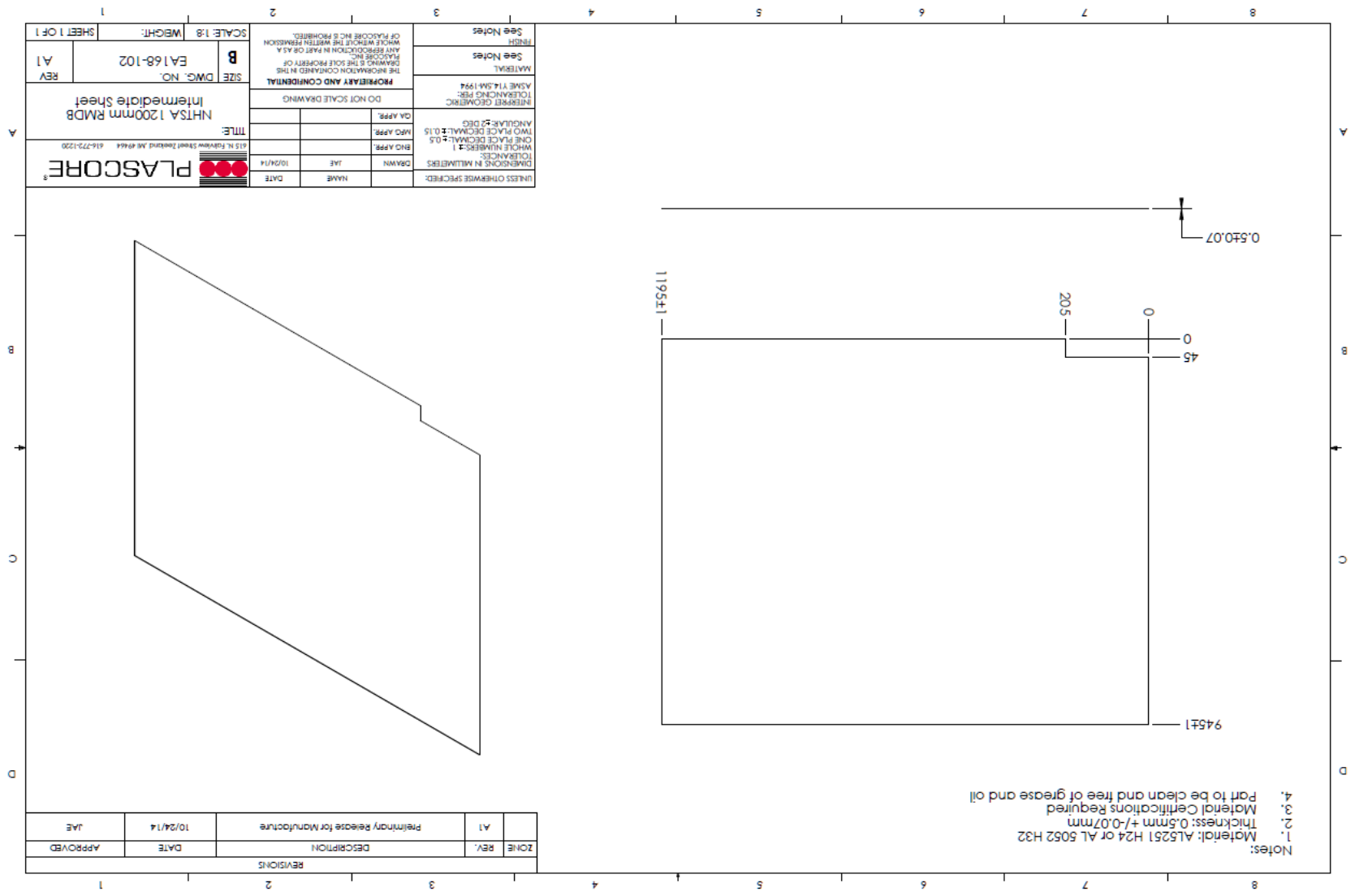


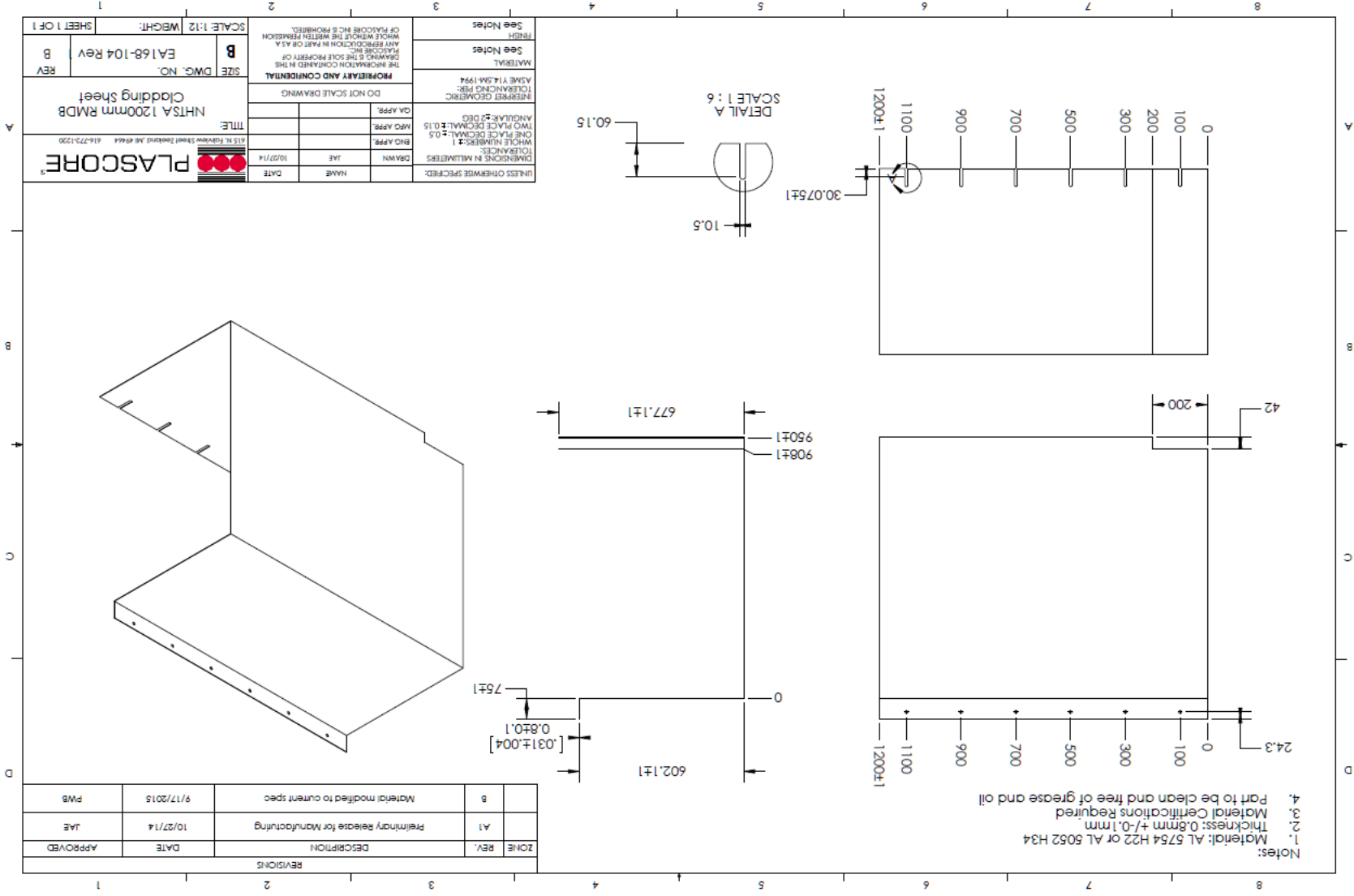
Figure 5 Bottom Flange Mounting Slots

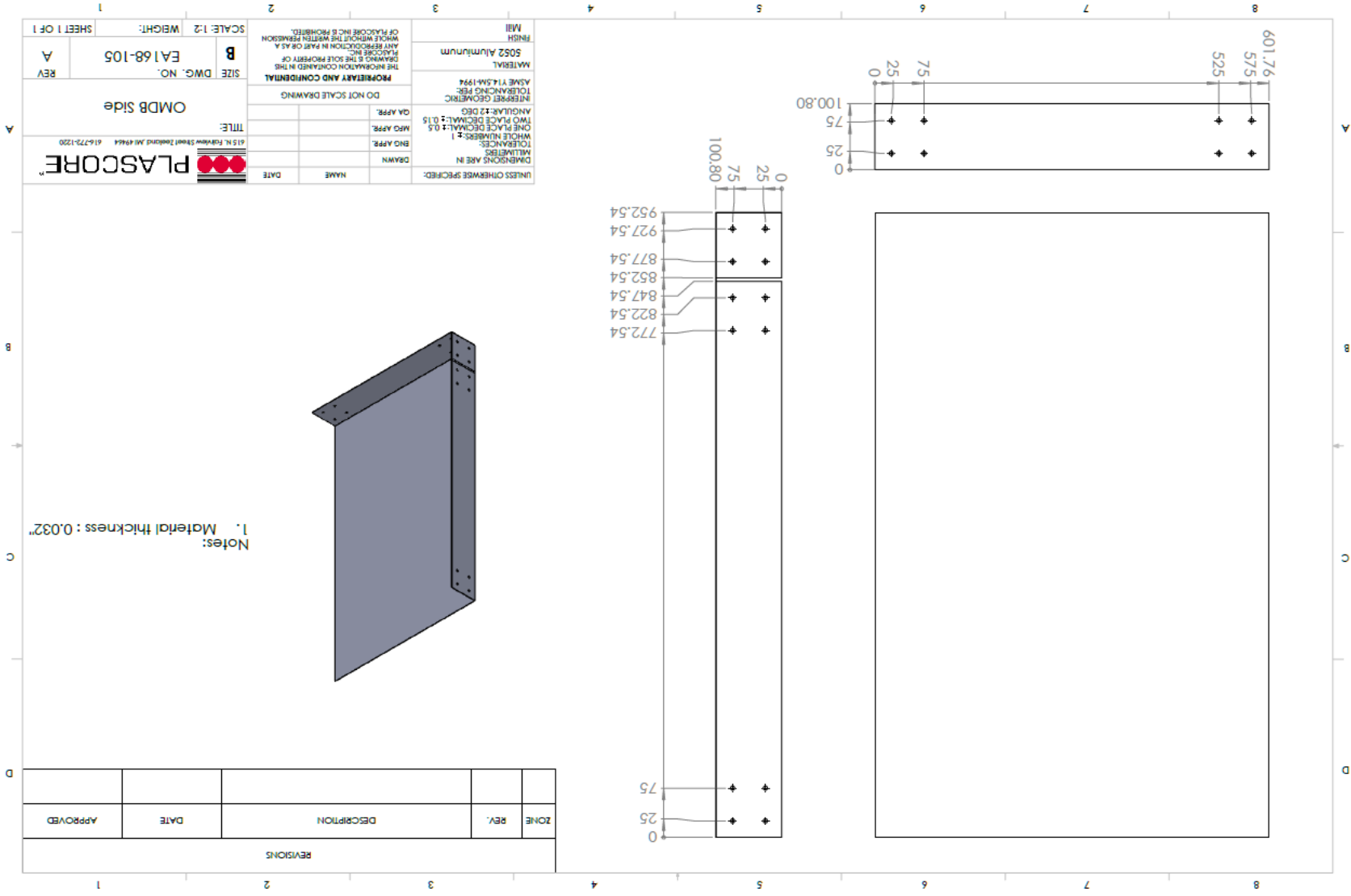
6.0 ASSEMBLY AND COMPONENT DRAWINGS

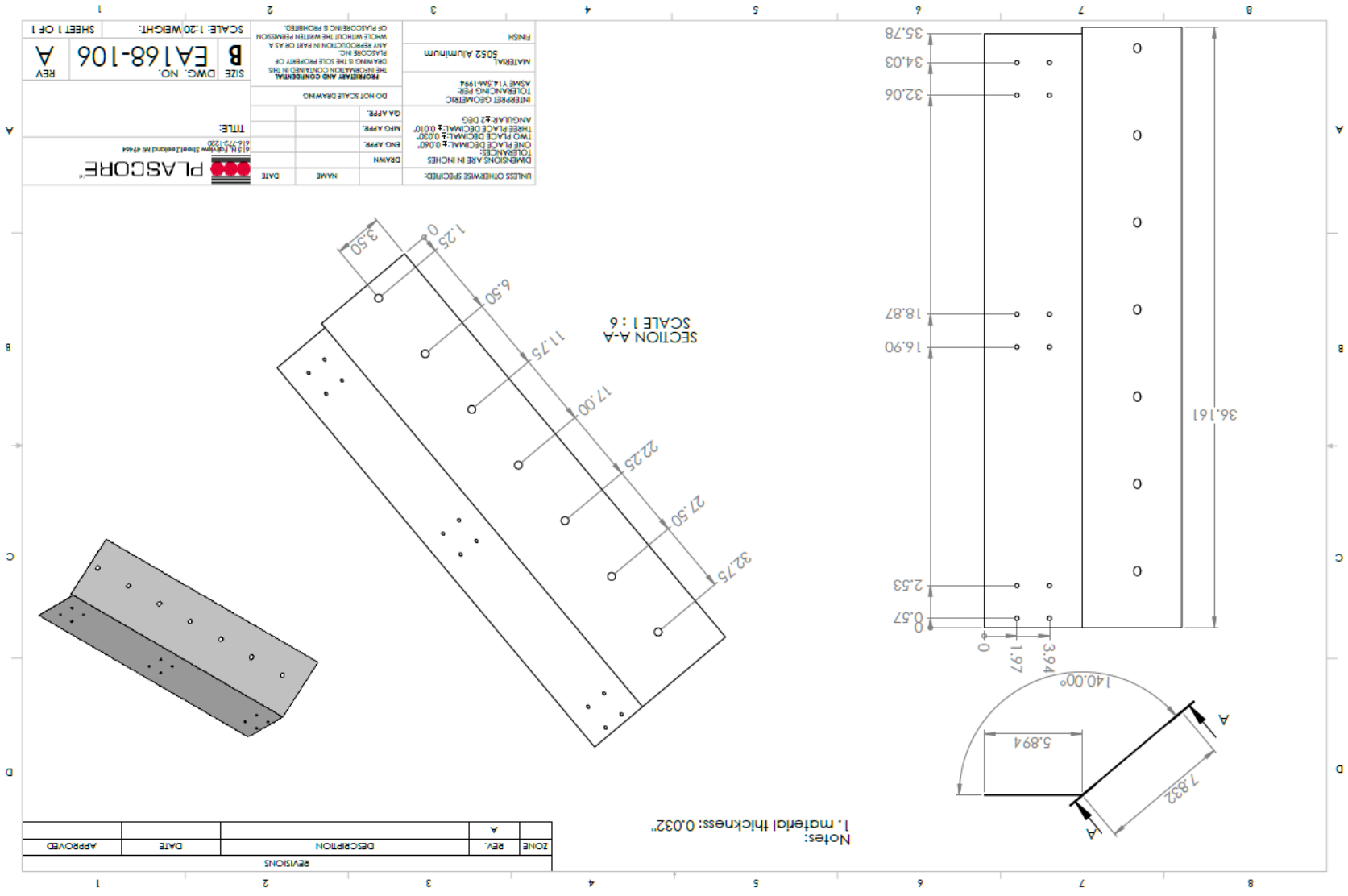
The following pages show dimensioned drawings for the components and the assembly of the NHTSA Oblique Moving Deformable Half Barrier Face V2019

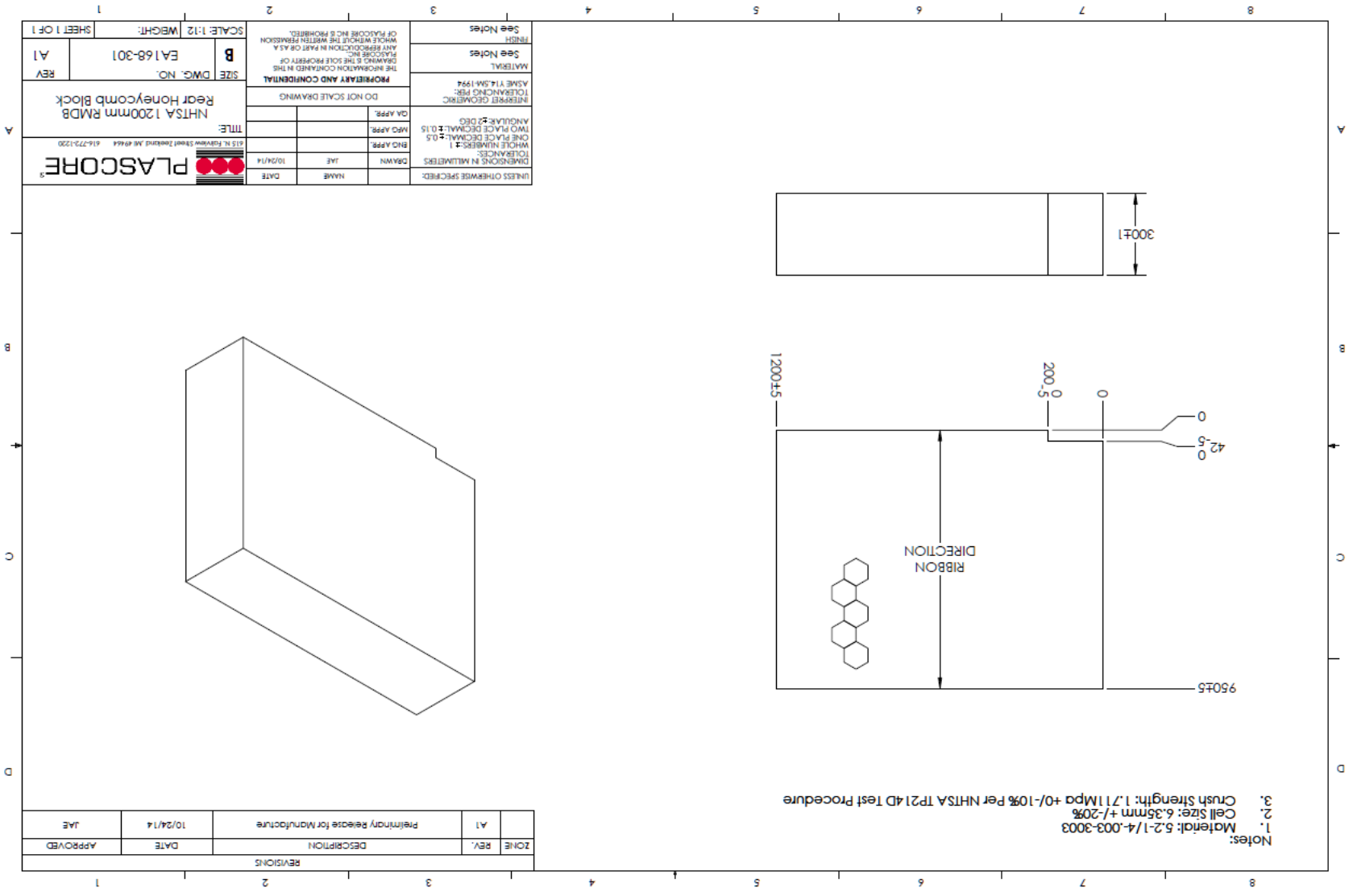












Notes:
 1. Material: 5.2-1/4-003-3003
 2. Cell Size: 6.35mm +/-20%
 3. Crush Strength: 1.711MPa +/-10% Per NHTSA TP214D Test Procedure

REVISIONS		
ZONE	REV.	DESCRIPTION
	A1	Preliminary Release for Manufacture
		DATE: 10/24/14
		APPROVED: JAE

UNLESS OTHERWISE SPECIFIED:		DRAWN	JAE	10/24/14
DIMENSIONS IN MILLIMETERS		DATE	NAME	DATE
WHOLE NUMBERS				
ONE PLACE DECIMAL: 0.5				
TWO PLACE DECIMAL: 0.15				
ANGULAR: 5 DEGS				
PREFER GEOMETRIC TOLERANCING PER: ASME Y14.5M-1994				
MATERIAL:				
FINISH:				
See Notes				
See Notes				
DO NOT SCALE DRAWING				
PROPERTY AND CONFIDENTIAL				
THE INFORMATION CONTAINED IN THIS DRAWING IS THE SOLE PROPERTY OF PLASCORE INC. ANY REPRODUCTION IN PART OR AS A WHOLE WITHOUT THE WRITTEN PERMISSION OF PLASCORE INC. IS PROHIBITED.				
SCALE: 1:12	WEIGHT:			
SIZE: B	DWG. NO.: EA168-301			
REV: A1				
TITLE: NHTSA 1200mm RMDB Rear Honeycomb Block				
PLASCORE				
615 N. FOWLER STREET, TAMPA, FL 33604 813-272-1200				

1 2 3 4 5 6 7 8 A B C D

